Chapter 4 Propulsion

From the standpoint of atmospheric flight, thrust is one of the four principal forces with which the engineer is likely to be familiar. (The other three principal forces are lift, drag, and weight.) Rockets are unique in this regard, because all nonwinged launch vehicles must use their engine(s) to produce both lift and thrust. Generally speaking, a *propulsive element* can be defined as any assemblage of components that is designed to impart an acceleration to the launch vehicle in order to change its position or velocity with respect to a frame of reference. The rocket engine that accelerates a launch vehicle upwards towards its final orbit is the most obvious example, although reaction control thrusters are also generally considered propulsive elements. Note that some devices, such as reaction wheels, change a vehicle's *orientation* with respect to a reference frame, but not its position or velocity with respect to that reference frame; as such, they are not considered propulsive elements and are not discussed here.

As is the case with other aerospace vehicles, the mission requirements of "how much," "how far," and "how fast" will constrain the design space of the propulsion system. Launch vehicles are also likely to encounter additional constraints that are unique among aerospace vehicles; these constraints usually deal with the large amount of thrust required to deliver a relatively small amount of payload to orbit (which drives weight fractions and performance requirements), as well as the extreme toxicity of several propellants. This toxicity not only impacts the performance of the propulsion system (due to chemistry and thermodynamics), but also drives material selection (due to corrosion) and storage and handling of propellants. The notion of propellant toxicity should not be taken lightly: jet fuel, for instance, can be safely handled with a minimum of protective equipment; should a few drops spill onto the ground (or onto the unlucky technician who's fueling the aircraft), the spill can be mitigated fairly easily. By contrast, spilling a few drops of hydrazine can result in liver and kidney damage, seizures, and death. Once consideration of propellant toxicity is taken into account, other real-world factors—specifically, the economy and lifecycle considerations of a launch vehicle design—become immediately relevant, rather than being a deprioritized, "also-need" design feature.

Several types of propulsive elements will be covered in this chapter. This chapter is devoted to chemical rockets (i.e., rockets that use combustion to provide thrust), because at the time of this writing they are still the most common form of propulsion for launch vehicles. Because chemical rockets derive their performance chiefly from the combustion of their propellants, an overview of the combustion process is presented first; this overview is by no means extensive, and the interested reader is directed to [1, 2, 3] for a more in-depth treatment of the subject.

A note on terminology: the word *engine* is typically used to refer to propulsive elements that "breathe" air (or oxygen) as part of the combustion cycle. For launch vehicles, the term *engine* refers to liquid architecture propulsive units (e.g., LOx/RP-1), whereas the term *motor* is reserved for propulsive units that utilize solid propellant. A propulsive unit that utilizes some combination of solid, liquid, or gaseous propellants is known as a *hybrid rocket*. Although the Oxford English Dictionary defines *motor* as a machine that supplies motive force (and motive force is certainly something that launch vehicles have in ample supply), the terminology used herein differentiates between the terms in accordance with current standard practice within the industry.

4.1 Combustion

Chemical rockets are unique among aerospace propulsion solutions in that the chemical rocket is typically not an air-breathing engine (because there is no sensible "air" above about 100 km or at orbital altitudes), and thus must carry its own "air" (in the form of an oxidizer) with it throughout its flight. This not only adds to the all-up mass of the launch vehicle, but also opens new design spaces for the propulsion engineer: after all, a jet engine is forced to breathe whatever composition of air is immediately available (regardless of its designer's wishes), but the designer of a chemical rocket can, during the design phase, tailor the performance of the vehicle's oxidizer to a certain degree. These propellants are consumed during flight, and it is the mechanics of combustion that impart to the launch vehicle the necessary momentum to perform its mission.

The calculation of the total temperature of a working fluid experiencing combustion under conditions of constant total pressure is a useful tool to predict the behavior of the combustion products as they enter the nozzle; as such, the majority of this section will be devoted to calculating this parameter. *Combustion* refers to the high-temperature chemical reaction that occurs between two elements, which produces heat (usually in the form of a flame). The entire purpose of combustion is to convert chemical energy (stored within the molecules of the propellants) into thermal energy, which can then be used to generate thrust. Within a launch vehicle's engine, these chemical elements are the propellants (which may be in solid, liquid, or gaseous form), which when combusted produce gaseous products. Once a specific amount of energy (called the *activation energy*) is supplied to the chemicals, a reaction can be sustained. The chemicals that "enter" a reaction are called *reactants*, whereas the results of a chemical reaction are called the *products* of the reaction.

Flames are classified according to three characteristics: the composition of the reactants, the character of the flame, and the steadiness of the flame.

The first characteristic, the composition, identifies the composition of the reactants upon entering the reaction zone. If the reactants are uniformly mixed together (or very nearly so), the flame is called *premixed*; otherwise, it is known as a *diffusion* flame, because the mixing of the propellants is accomplished via diffusion. The second characteristic identifies whether the flame is laminar or turbulent; for laminar flames (i.e., those occurring at low Reynolds numbers) the mixing and transport are accomplished through purely molecular processes, whereas turbulent flames (i.e., those occurring at high Reynolds numbers) substantially enhance the mixing and transport phenomena via macroscopic turbulent phenomena (e.g., eddy flow). The third characteristic of a flame identifies whether it is steady or unsteady, determined by whether the flame structure changes relative to the initial phase of the reactants.

To simplify the design cycle of propulsion systems, a number of assumptions must be made with regard to combustion. These assumptions are commonplace and are especially prevalent in classical combustion models:

- Reacting fluid is a continuum.
- Chemical equilibrium (stoichiometry) is always attained.
- Chemical reactions occur infinitely fast.
- Chemical reactions are irreversible.
- Ideal gas assumptions are valid.
- All species have equal mass diffusivity.
- Lewis, Schmidt, and Prandtl numbers are approximately unity.
- Fick's law of diffusion is valid.
- All gas phases have constant specific heats.
- Reacting solid surfaces are energetically homogeneous.
- Low-speed combustion occurs at uniform pressure.
- Dufour effect (energy flux due to mass concentration gradient) and thermophoresis (Soret effect, wherein particle types in a mixture exhibit different responses to thermal gradients) are negligible.
- When flowing through a nozzle, all chemistry is assumed "frozen" (i.e., having an infinitely slow reaction rate).

Despite the often-complicated sequence of chemical reactions that occurs during combustion, it is important to remember that the heat produced by combustion often makes the combustion self-sustaining. Combustion also requires fairly high temperatures, especially when catalysts (substances that increase the rate of chemical reactions without undergoing significant chemical changes themselves) are not used. Combustion is said to be "complete" when it is *stoichiometric*—that is, when there is no remaining fuel, there is also no remaining oxidant. In addition, stoichiometry implies that the products of a chemical reaction are stable. In practice, this chemical equilibrium is virtually impossible to achieve; therefore, complete combustion is similarly difficult to achieve. Real combustion reactions often contain unburned reactants that are carried off by the products of the combustion (e.g., smoke), which means that these products will usually be toxic. Unburned reactants, by definition, have not undergone combustion, and have therefore contributed nothing to the overall energy output of the engine; thus, attaining and maintaining chemical equilibrium while minimizing the amount of unburned reactants is a crucial effort in the design of rocket engines.

Note that for any combination of fuel and oxidizer used, the ratio of fuel to oxidizer (commonly denoted as f) that results in a stoichiometric reaction is unique. Note that the ratio of fuel to oxidizer is always given in terms of units of **mass**, not units of volume. It is often beneficial to describe the fuel–oxidizer mixture in terms of this unique stoichiometric ratio, typically through the use of an *equivalence ratio*, commonly referred to as φ

$$\varphi = \frac{f}{f_{\text{stoich}}} \tag{4.1}$$

where f_{stoich} represents the stoichiometric fuel–oxidizer ratio. For $\varphi < 1$, the mixture is said to be fuel-lean (oxidizer-rich), whereas $\varphi > 1$ denotes a fuel-rich (oxidizer-lean) mixture. Combustion behavior is very dependent on equivalence ratio and flame temperature, and these terms have a very real impact on the performance of an engine. A lean mixture, for instance, will typically result in a lower combustion temperature, but a rich mixture of hydrocarbon fuel can produce soot or oxides of nitrogen within certain temperature regimes.

Another useful fuel metric is known as *bulk density*, which is a measure of the density of the individual propellants relative to the total volume they occupy; it can be thought of as the "average" density of the mixed propellant, and is defined as

$$\rho = \frac{f + 1}{\dfrac{f}{\rho_f} + \dfrac{1}{\rho_o}} \tag{4.2}$$

Note that the bulk density is entirely and only dependent upon both the individual densities of the oxidizer (ρ_o) and fuel (ρ_f), as well as the oxidizer–fuel ratio. Generally speaking, a higher propellant bulk density will result in smaller propellant tanks.

The maximum possible flame temperature for a combustion reaction is known as the *adiabatic flame temperature*, and is the temperature that a flame reaches if there is no energy lost to an external environment. This flame temperature is usually reached at equivalence ratios between 1.0 and 1.1, although it should be noted that the adiabatic flame temperature (which usually ranges from 2,000 to 5,000°C or 3,600 to 9,000°F) is *theoretical*, and that material properties will usually limit the maximum operating temperature of an engine. Additionally, a limit on flame temperature may be imposed due to the fact that some products of chemical reactions will, at sufficiently high temperature, begin to dissociate back into their constituent reactants. The implications of this will be discussed later in this section.

The gases that comprise the combustion "charge" (also known as the working fluid) can, for the purposes of initial design, be treated as ideal gases. There are various forms of the ideal gas law, which relates the gas pressure P, gas volume V, gas mass m, and gas temperature T through the use of a specific gas constant R or the universal gas constant $\mathcal{R}$ (8.314462 J/mol-K), and the molecular weight of the gas MW

$$PV = mRT = \rho RT = m\frac{\mathcal{R}}{MW}T = n\mathcal{R}T \tag{4.3}$$

Equation (4.3) is known as the equation of state of an ideal gas. Note that the specific gas constant is a function of the universal gas constant and the molecular weight of the gas,

$$R = \frac{\mathcal{R}}{MW} \tag{4.4}$$

and will therefore be different for different gases.

Recall from basic thermodynamics that the gas specific heat at constant volume c_v (also known as the isochoric specific heat) and the specific heat at constant pressure c_p (also known as the isobaric specific heat) are related by the specific gas constant

$$c_p - c_v = R \tag{4.5}$$

The behavior of a flowing gas is strongly influenced by its ratio of specific heats γ, which is simply

$$\gamma = \frac{c_p}{c_v} \tag{4.6}$$

4.2 The Thrust Equation and Rocket Equation

The thrust provided to a rocket can be derived from Newton's second law, $F = ma$. Converting this to a more immediately applicable form and defining momentum as the product of mass and velocity, $p = mv$,

$$\begin{aligned} F &= ma \\ F &= \frac{\mathrm{d}p}{\mathrm{d}t} \\ F &= m\frac{\mathrm{d}v}{\mathrm{d}t} \\ F &= v\frac{\mathrm{d}m}{\mathrm{d}t} \end{aligned} \tag{4.7}$$

In rocketry, this final form of $F = ma$ is usually written as $F = \dot{m}v_e$, indicating that thrust is proportional to the mass flow rate of propellants (fuel and oxidizer) multiplied by the exit velocity of the combusted propellants, which for initial design may be assumed constant. This *jet thrust*, or *momentum thrust*, is produced solely by the expulsion of combusted propellant mass from the rocket nozzle (Fig. 4.1). A more accurate form of thrust must also include contribution from the exhaust pressure acting on the exit plane of the nozzle; this is commonly known as the *thrust equation*,

$$F = \dot{m}v_e + (P_e - P_\infty)A_e \tag{4.8}$$

where P_e and P_∞ are, respectively, the exit pressure of the nozzle and the freestream pressure of the surrounding atmosphere, and A_e is the cross-sectional exit area of the nozzle. The total thrust is the sum of the momentum thrust less the pressure losses acting upon the nozzle exit plane (Fig. 4.1). The pressure term from the rocket equation represents the pressure loss incurred when the exhaust flow is not properly expanded.

Generally speaking, the momentum term ($\dot{m}v_e$) is much greater than the pressure term (the pressure term is a small percentage of the momentum term or less), and can often be neglected. It should also be apparent that, with conventional nozzles, it is possible to ideally expand the exhaust flow at only one flight condition (that being where the exhaust pressure Pe is equal to the freestream pressure P_∞); at every other flight condition, the exhaust flow will be either over- or underexpanded, as shown in Fig. 4.2. As seen in Fig. 4.3, the difference in thrust from Apollo 11 due to properly expanding the exhaust flow was on the order of 5,500 kN, which is certainly not insignificant!

It should be immediately obvious that there are only so many "knobs to turn" to increase thrust. Increasing the pressure of the combustion chamber is certainly possible, although this will also increase the combustion temperature and therefore affect the oxidizer–fuel ratio. Increasing the mass flow rate of the propellants increases the momentum term and will provide a

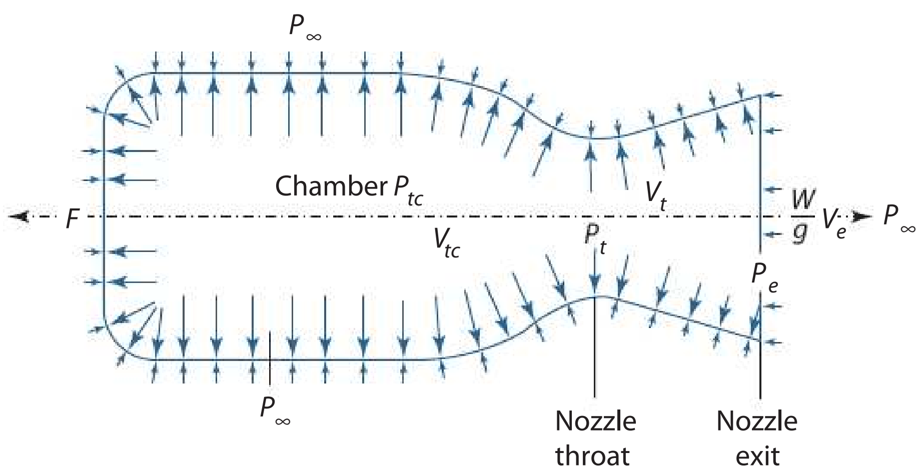

Fig. 4.1 Rocket thrust control volume.

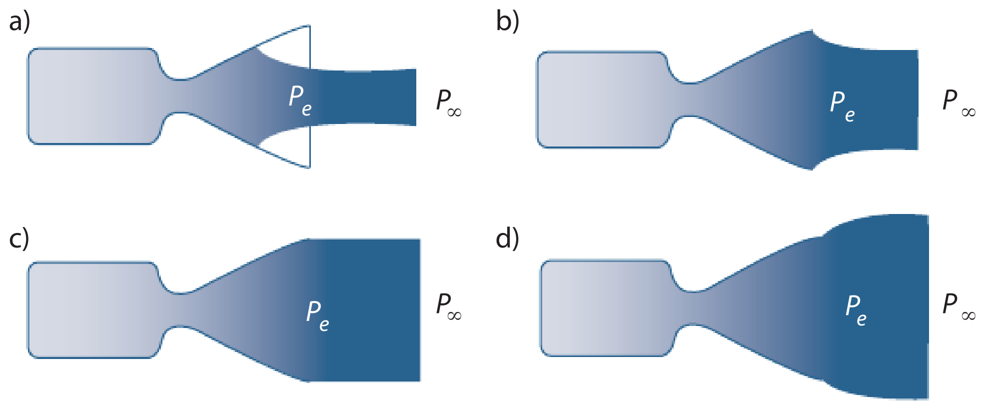

Fig. 4.2 a) Grossly overexpanded flow; b) overexpanded flow; c) ideally expanded flow; d) underexpanded flow.

much higher effect on the thrust produced; however, only so much propellant can be carried for a given mission. Properly expanding the flow such that the pressure term becomes zero will certainly increase thrust, but the change will be both negligible and applicable at only one flight condition, because the freestream pressure will constantly change during the vehicle's ascent. (The exception to this is the aerospike engine, which is discussed later in

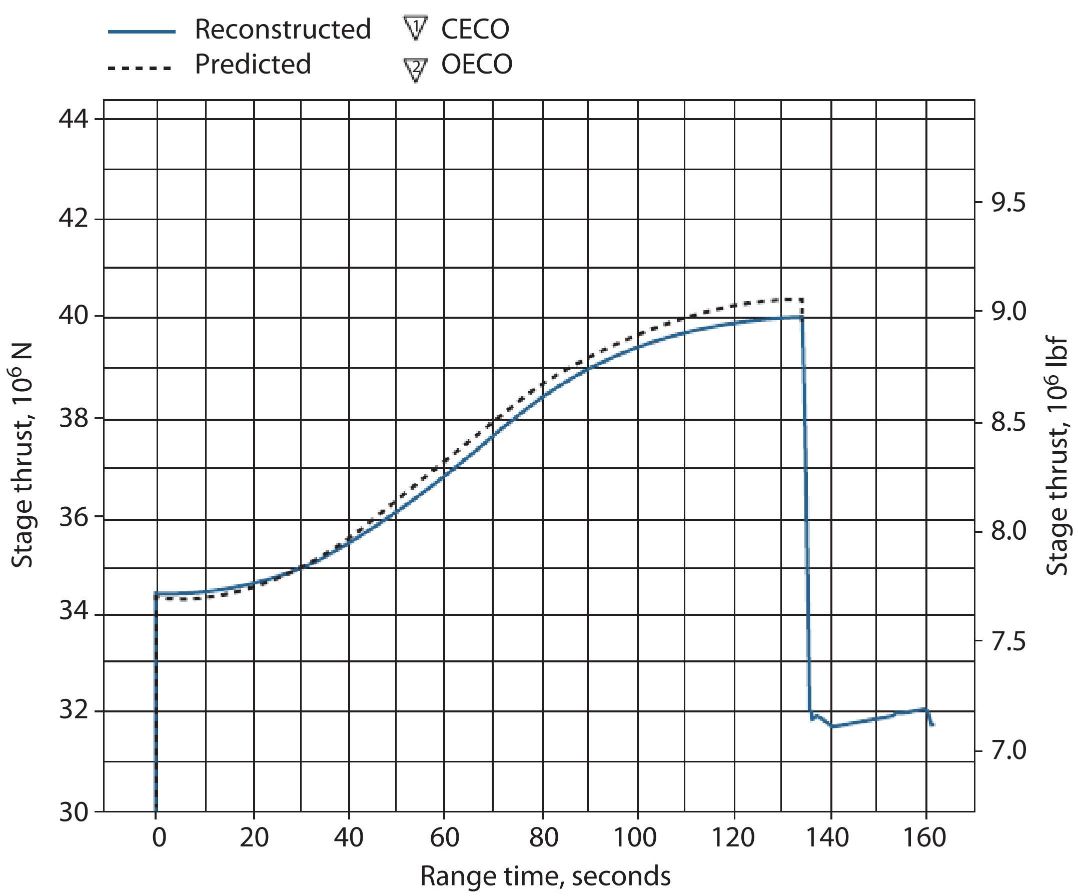

Fig. 4.3 Thrust increase from ambient pressure drop, Apollo 11. Source: NASA.

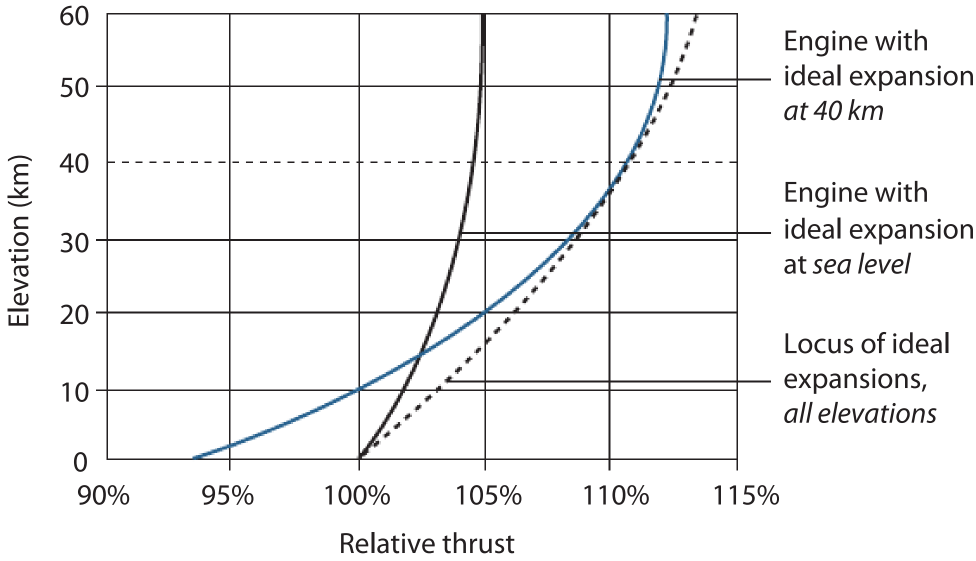

Fig. 4.4 Thrust vs altitude for various nozzle expansions. Source: [4].

the chapter.) Ideally, the nozzle should be designed to yield ideal expansion at approximately two thirds of the total flight altitude desired, which will yield more favorable thrust throughout the flight than a nozzle that ideally expands the flow at sea level (Fig. 4.4).

4.2.1 Exhaust Velocity

It has been shown that the exhaust velocity, along with the mass flow rate of propellant(s), is the key driver in the total amount of thrust that can be produced by a rocket engine. The average ejected velocity (typically written v_e or U_e) is a function of the following five factors:

- Exhaust pressure P_e
- Combustion chamber total pressure P_0
- Combustion chamber total temperature T_0
- Exhaust gas molecular weight MW
- Ratio of specific heats of combustion product γ

Thus, the thermochemistry of the propellants must be known. The total temperature of the combustion chamber depends on the total temperature and enthalpy of the propellant mixture, as well as the oxidizer–fuel ratio and the isobaric gas constants of the reactants and products, as given earlier in the chapter. Thus, the exhaust velocity can be calculated as

$$v_e = \sqrt{\frac{2\gamma}{\gamma - 1}\frac{\mathcal{R}T_0}{MW}\left[1 - \left(\frac{P_e}{P_0}\right)^{\frac{\gamma-1}{\gamma}}\right]} \tag{4.9}$$

For an ideally expanded nozzle, the exhaust backpressure is approximately zero, and the exhaust velocity can be approximated as

$$v_e \cong \sqrt{\frac{2\gamma}{\gamma - 1}\frac{\mathcal{R}T_0}{MW}} \tag{4.10}$$

This approximation assumes that all of the thermal energy of the exhaust has been converted to kinetic energy, and thus the exhaust velocity is solely a function of combustion temperature and molecular weight of the combustion products. This also reveals another important point: the importance of molecular weight. As shown previously, a chemical reaction must be balanced; this means that the total mass of reactants prior to combustion must equal the total mass of products after combustion; however, it must also be noted that heavier, more complex fuels require more oxygen to combust (cf., methane vs hexane), and the molar mass of the products will also be heavier and more complex. This impacts the *molar efficiency* (i.e., total thrust produced per unit mass of propellant) of the vehicle. Higher molar mass equates to a lower exhaust velocity, and thus reduced thrust per unit mass of propellant. Therefore, a *lighter* fuel will, on the basis of molar efficiency, be preferable. Liquid hydrogen is favored as a propellant for precisely this purpose, although it is a cryogenic fuel and therefore not necessarily the best solution for every design when operating and cost constraints are considered. Regardless, it is generally preferable to use the lightest fuel possible for a given application, in order to maximize the thrust efficiency of the vehicle.

The exhaust velocity can also be rewritten as a *specific* exhaust velocity c, which is the total thrust divided by the mass flow rate of propellant

$$c = \frac{F}{\dot{m}} = v_e + \frac{A_e(P_e - P_\infty)}{\dot{m}} \tag{4.11}$$

which is, essentially, the total impulse of the rocket engine normalized by the mass flow rate. Rewriting the specific exhaust velocity in terms of Mach number at the exit plane of the nozzle,

$$c = v_e\left[1 + \frac{1}{\gamma M_e^2}\left(1 - \frac{P_\infty}{P_e}\right)\right] \tag{4.12}$$

For a large exhaust area with a high Mach number, the pressure term is a negligible portion of the overall thrust produced.

4.2.2 Rocket Performance: Total and Specific Impulse

A useful analysis tool is the total impulse I provided by the propellant, which is equal to the area under the thrust-time curve (if the thrust is constant, the total impulse is the thrust multiplied by the burn time):

$$I = \int_{o}^{t_b} F(t)\mathrm{d}t = F_{\mathrm{ave}} t_b \tag{4.13}$$

This is the *total impulse*, which is a measure of the momentum that can be supplied to the vehicle by combustion of the propellants. Solid propellant hobby model rocket motors are categorized by their total impulse on an alphabetic scale, i.e. an "A" motor has a total impulse between 1.26–2.5 Ns, a "B" motor has twice the total impulse, between 2.51–5.0 Ns, and so on, doubling with each successive letter of the alphabet. Under such a designation, the Mercury-Redstone rocket would have a classification of letter Z, between 41.9 and 83.9 $\times$ 10^6 (million) Ns!

The average thrust is defined as the total impulse divided by the burn time, or $T_{ave} = I_{tot}/t_b$. Hence the total impulse for a constant-thrust rocket is the thrust T_c (constant) multiplied by the burn time, or $I_{tot} = T_c\ t_b$.

We will also use a term called *specific impulse* defined as the amount of thrust produced per unit of propellant consumed per unit time. Specific impulse is a measure of the efficiency of a rocket engine, and *higher is better*.

In the English/Imperial system, propellant consumed (w_p) is measured by weight ($\mathrm{lb_f}$), and in the SI system, propellant consumed (m_p) is measured by mass (kg). Hence, if g_0 is the (standard) acceleration of gravity at Earth sea level ($g_0 = 9.80665\ \mathrm{m/s^2} = 32.17405\ \mathrm{ft/s^2}$), for the specific impulse in the two sets of units we have the following relations:

$$I_{sp-\mathrm{English}} = \frac{T}{w_p/t} = \frac{T}{\dot{w}_p} = \frac{T}{g_0 \dot{m}_p} = \frac{v_e}{g_0} \tag{4.14}$$

and

$$I_{sp-SI} = \frac{T}{m_p/t} = \frac{T}{\dot{m}_p} = v_e \tag{4.15}$$

Note that there is a difference in I_{sp} depending on the unit system used: the units of I_{sp} could be in *seconds* or in *meters per second*, depending on whether the Imperial or SI systems of units is used, respectively. The SI version of specific impulse happens to be particularly useful because it is precisely the engine's effective exhaust speed. (If the English/Imperial specific impulse also used its mass units of slugs, then its specific impulse would be the effective exhaust speed in ft/sec.)

In this text, I_{sp} will be given using both sets of units, either seconds (which is consistent with U.S. industry practice), or in meters/second (the rest of the world). The units will immediately indicate which system is being used. Typical I_{sp} values (Imperial units) for various propellants are given in Table 4.1. Table 4.1 indicates that the hydrogen + oxygen combination provides the highest value of specific impulse, which is related to its combustion

Table 4.1 Typical Specific Impulse Values

Propellants	Application	Exhaust Products	I_{sp}, s
Black powder	Amateur rocketry	(various)	80
Zinc, sulfur	Amateur rocketry	ZnS	240
Al, NH_4ClO_4	Shuttle SRM	(various)	287
Hydrazine, RFNA	OMS, Titan	H_2O, NH_3	313
Ethyl alcohol, LOx	V-2	H_2O, CO_2	330
RP-1, LOx	Atlas V, Saturn IC	H_2O, CO_2	350
Methane, LOx	(various)	H_2O, CO_2	370
LH_2, LOx	Delta IV, Space Shuttle	H_2O	450

product's low molecular weight. But is this the "best" propellant? Practical considerations make this theoretical best propellant combination less desirable. For example:

A) LH_2's density is about an order of magnitude less than most other fuels at 70 kg/m^3 (i.e. RP-1 at 820 kg/m^3 and LCH_4 at 416 kg/m^3). This leads to larger tanks and structures to accommodate the added volume of propellant needed.
B) The temperature needed for storing LH_2 is near absolute zero, meaning more tank insulation mass.
C) Other issues such as the difficulty of sealing against hydrogen leakage, and hydrogen embrittlement of the tank walls.

These all lead to more complex issues and higher costs associated with manufacturing, handling, and transportation of the launch vehicle structure as well as with storage and loading of LH_2 fuels. We recommend that the designer consider these issues when choosing a propellant combination.

The specific impulse of a propellant can also be used to determine the overall size of the launch vehicle through the use of *volumetric specific impulse,* usually written as $I_{sp_{\mathrm{vol}}}$, which is equal to the specific impulse multiplied by the specific gravity of the propellant

$$I_{sp_{\mathrm{vol}}} = I_{sp}SG \tag{4.16}$$

The *higher* the volumetric specific impulse is, the *less* space will be needed to store the propellants, which in turn equates to a smaller (and likely lighter) launch vehicle. For a fixed volume and mass, increasing the volumetric specific impulse increases the velocity increment delivered during flight. A very high volumetric specific impulse is desirable for the first stage of a multistage launch vehicle, in order to minimize both weight and aerodynamic penalties; if this cannot be achieved, strap-on boosters are often an economical way to increase the payload fraction of the launch vehicle. Typical

Table 4.2 Typical Sea-level and Vacuum Volumetric Specific Impulse Values

Propellant	Sp. Gravity (Density, kg/m^3)	Sea Level I_{sp} (s)	Sea Level I_{sp-Vol} (s)	Vacuum I_{sp} (s)	Vacuum I_{sp-Vol} (s)
LOX/Kerosene (*Saturn V* F-1)	1.3 (1,300)	265	**345**	304	**395**
LOX/LH_2 (*Saturn V* J-2)	0.28 (280)	360	101	424	119
LOX/LH_2 (Shuttle SSME)	0.28 (280)	390	109	455	127
Solid Propellant (Shuttle SRM)	1.35 (1,350)	242	**327**	262	**354**

volumetric specific impulse values for the Saturn V and Space Shuttle are given in Table 4.2. Notice that hydrolox volumetric specific impulses are a factor of three or four lower than those of kerolox, meaning the former will need much larger tanks than the latter.

Three other factors govern a rocket's specific impulse: oxidizer–fuel ratio (mixture ratio), chamber pressure, and expansion ratio (ratio of exit area A_e to throat area A_t), as shown in Fig. 4.5b. As can be seen, the specific impulse will usually depend more on the expansion ratio of the nozzle than on the

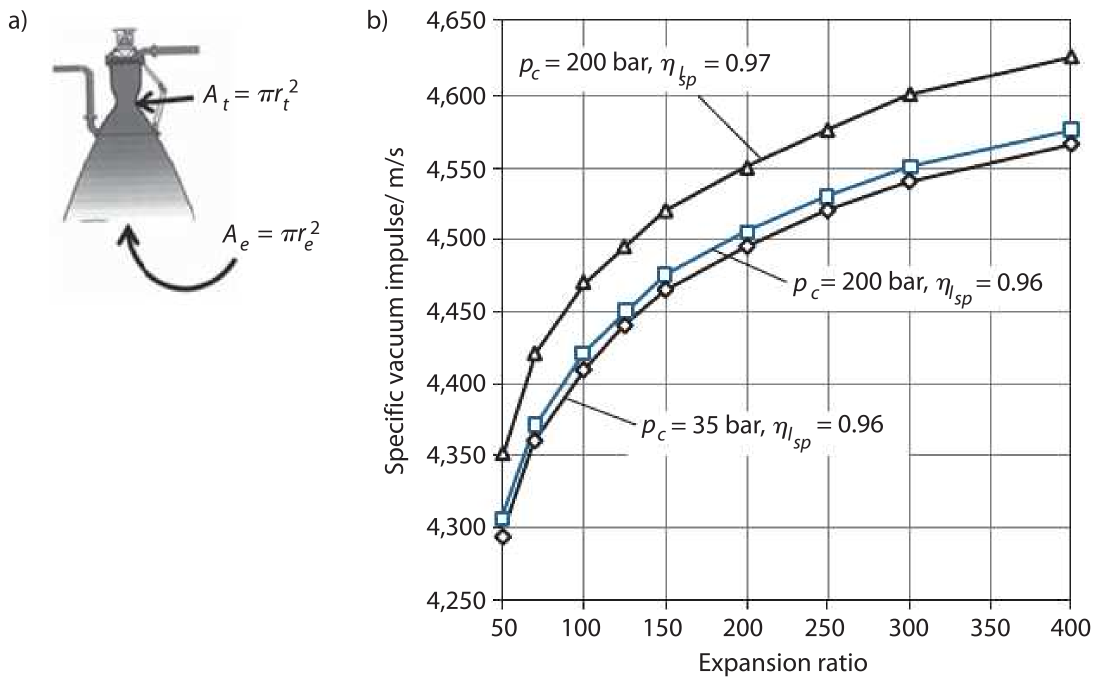

Fig. 4.5 Specific impulse as a function of nozzle expansion ratio and chamber pressure. (a) Nozzle throat (t) and exit (e) dimensions; (b) I_{sp} vs chamber pressure expansion ratio. Source: Ley et al. [5].

chamber pressure. This would lead one to conclude that larger nozzles are more desirable. Generally speaking, this is true; however, incorrectly expanding the nozzle results in detrimental effects on the thrust produced, as discussed previously.

Specific impulse also changes as a function of the oxidizer–fuel ratio of the propellant, as shown in Fig. 4.6. It should be immediately apparent that, for any combination of fuel and oxidizer used as propellants, there exists an optimum oxidizer–fuel ratio for which the I_{sp} will be at a maximum. The engine itself may not be able to *operate* at this oxidizer–fuel ratio (due to other considerations, such as thermal limits, performance of pumps, etc.), but the specific impulse does not increase without bound as the oxidizer–fuel ratio increases.

The engine's mixture ratio describes the amounts of fuel and oxidizer that are injected into the engine. Two different expressions are commonly used: *r*, the *Oxidizer-to-Fuel* mixture ratio, and *f*, *Fuel-to-Oxidizer* mixture ratio. Either of these expressions may be used to calculate the *bulk density* of the entire load of fuel in a vehicle, where the bulk density is defined as the average density of the two propellants and may be used to calculate the total propellant volume needed. Of course, that total volume would be broken into a volume for each of the propellants; this procedure is described

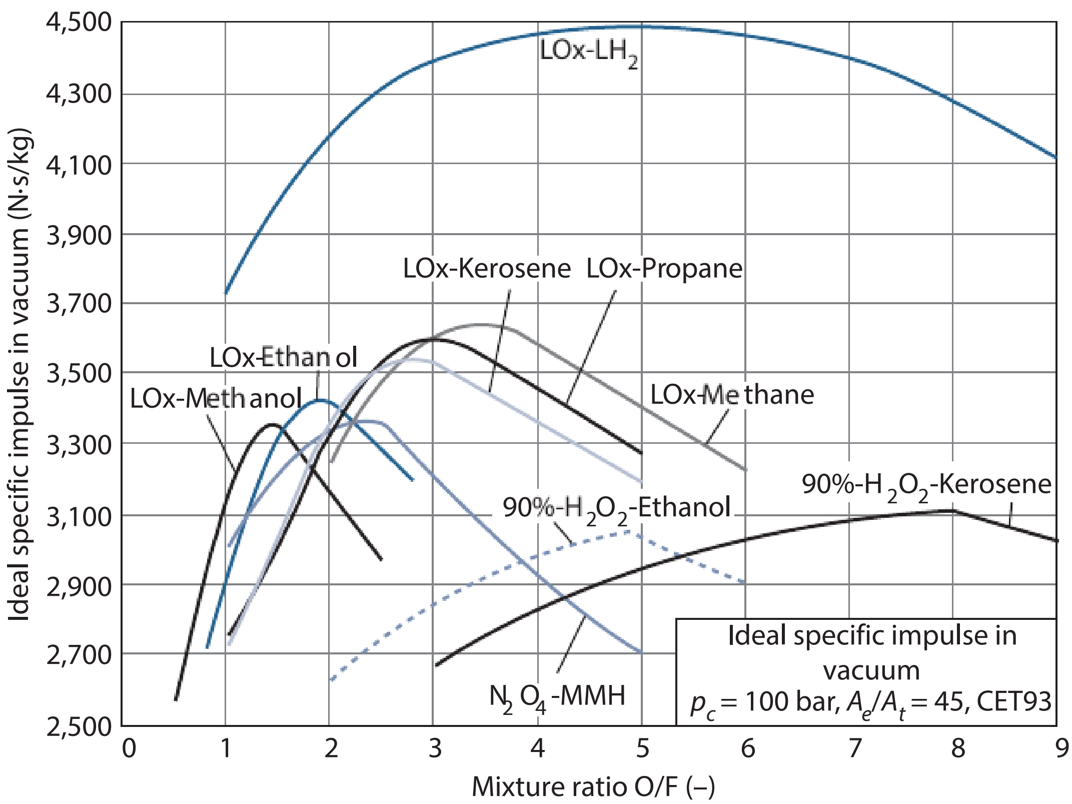

Fig. 4.6 Specific impulse as a function of propellant type and oxidizer–fuel ratio. Source: Ley et al. [5].

Table 4.3 Relationships Between Propellant Mix Ratios and Bulk Density

Mix Type	Definition	Bulk Density
r, Oxidizer-to-Fuel Mixture Ratio (*Ox/F* ratio)	$r = \frac{\dot{m}_{oxidizer}}{\dot{m}_{fuel}}$	$\rho_{bulk} = \frac{r+1}{\frac{r}{\rho_{ox}} + \frac{1}{\rho_f}}$
f, Fuel-to-Oxidizer Mixture Ratio (*F/Ox* ratio)	$f = \frac{\dot{m}_{fuel}}{\dot{m}_{oxidizer}}$	$\rho_{bulk} = \frac{f+1}{\frac{f}{\rho_f} + \frac{1}{\rho_{ox}}}$

in Chapter 8, Vehicle Sizing. The relationships between the mix ratios are given in Table 4.3.

To calculate the performance of a launch vehicle in an atmosphere, we need to take into account the variation of specific impulse with altitude. A typical variation of this parameter is shown in Fig. 4.7. The effective value of the specific impulse is the area under the flat line shown in the figure which has the same area as that under the I_{sp} curve. For many vehicles, a useful approximation is found in [6]

$$I_{sp-eff} = \frac{2}{3} I_{sp-vac} + \frac{1}{3} I_{sp-SL} \tag{4.17}$$

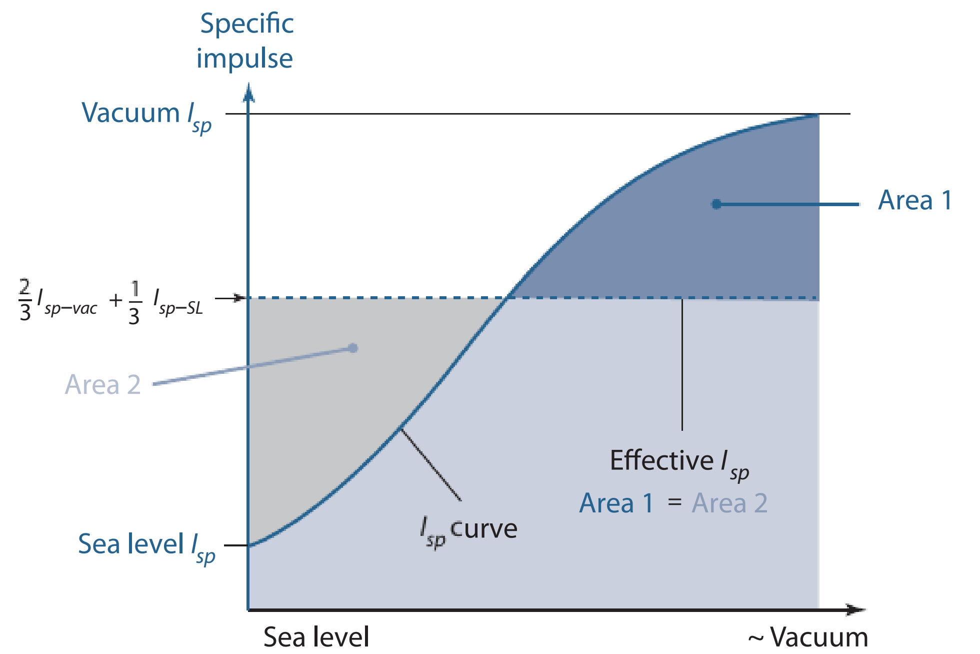

Fig. 4.7 Effective specific impulse considers the variation in I_{sp} with time or altitude. A recommended value is $I_{sp-eff} = \frac{2}{3} I_{sp-vac} + \frac{1}{3} I_{sp-SL}$.

Similarly, one can calculate the effective exhaust velocity c_{eff} using

$$c_{eff} = \frac{1}{3}\, c_{SL} + \frac{2}{3}\, c_{vac} \tag{4.18}$$

4.3 The Rocket Equation

The ultimate performance requirement for any launch vehicle or spacecraft is the change in velocity Δv (as discussed in Chapter 3), and is given as the *Tsiolkovsky rocket equation*, or

$$\Delta v = g_0 I_{sp-\text{English}} \ln \frac{m_0}{m_f} = v_e \ln \frac{m_0}{m_f} \tag{4.19}$$

where m_0/m_f is called the *mass ratio* (usually given as μ or MR) and refers to the initial mass of the launch vehicle (typically its gross liftoff mass, or GLOM) divided by the final mass of the system (typically the mass of everything except the consumed propellants). Generally speaking, a higher mass ratio is more desirable, because it indicates that more of the rocket's all-up mass is "useful" (i.e., less inert mass). The rocket equation can, therefore, be applied to multiple-stage or single-stage launch vehicles with equal ease. The first form of the rocket equation is typically more useful in design, because the specific impulse of various propellant combinations can often be found in tables, whereas the exhaust velocity of a motor is typically not known before the motor has been designed. Note that the gravitational constant is equal to the standard value of 9.80665 $\mathrm{m/s^2}$ no matter where the Δv is being calculated.

4.3.1 Propellant Mass Fraction and Total Impulse

Occasionally, a *propellant mass fraction* is used, especially for situations requiring multiple burns of varying durations or thrust levels, such as multiple burns of an upper- or lower-step engine. This propellant mass fraction is given as

$$\zeta_p = \frac{m_p}{m_0} \tag{4.20}$$

where m_p is the mass of the propellant and m_0 is the all-up mass of the vehicle prior to the burn. Note that the propellant mass fraction only accounts for the amount of usable propellant, and does not account for residual propellant, which is never consumed.

Rarely are propellant tanks fully filled; instead, as shown in Fig. 4.8, there is usually "ullage space" for a pressurizing gas to enter the propellant tank.

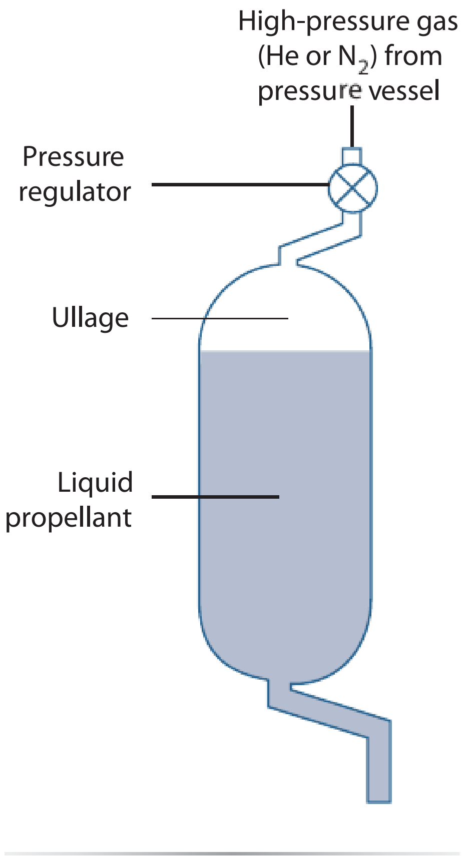

Fig. 4.8 Typical arrangement of liquid propellant with ullage space for pressurizing gas.

Note that

$$MR = \mu = \frac{1}{1 - \zeta_p} \tag{4.21}$$

and

$$\zeta_p = 1 - \frac{1}{\mu} \tag{4.22}$$

Typical propellant mass fractions are in the range of approximately 90%.

4.3.2 Thrust-to-weight ratio and burn time

The thrust to weight ratio of the rocket is equal to the total thrust produced divided by the all-up mass of the rocket:

$$\frac{T}{W} = \frac{T}{m_0 g_0} \tag{4.23}$$

This can be related to the mass flow rate of propellant and the specific impulse of the rocket by

$$\frac{T}{W} = \frac{\dot{m}_p c}{m_0 g_0} = \frac{\dot{m}_p I_{sp}}{m_0} \tag{4.24}$$

Thus, for a given engine or motor, the higher the exit Mach number, the higher the propellant mass flow rate, and the higher the specific impulse, the greater the thrust-to-weight ratio of the rocket. Higher values of T/W are preferred, but a $T/W > 1$ is required for the rocket to be able to lift off at all.

The initial thrust-to-weight ratio is usually defined as

$$\frac{T}{W_0} = \psi_0 \tag{4.25}$$

For the purposes of initial design, the propellant mass flow rate can be averaged by dividing the total mass of the available propellant by the burn time, t_b:

$$\dot{m}_p = \frac{m_p}{t_b} \tag{4.26}$$

This equation reveals a useful design metric. Solving for the burn time and using the definitions of propellant mass fraction and specific impulse,

$$t_b = \frac{\zeta_p I_{sp}}{T/W_0} = \frac{\zeta_p I_{sp}}{\psi_0} \tag{4.27}$$

The propellant mass fraction, ζ_p, must always be less than one (rockets are rarely just propellant devoid of *any* structure); conversely, the thrust-to-weight ratio must always be greater than one (in order to lift off). Therefore, the theoretical burn time, in seconds, can never be greater than the English or Imperial (weight-normalized) specific impulse!

Example 4.1 Spacecraft with a partial burn cycle

A spacecraft with the following properties combusts a portion of its propellants. Find 1) the exhaust velocity, 2) the specific impulse, 3) the total impulse, and 4) the propellant mass fractions before and after the burn.

Item	Value
Total spacecraft mass	27,320 kg
Propellant mass before burn	1,521 kg
Propellant mass after burn	862 kg
Burn time	2 sec.
Δv	56 m/s

To find the exhaust velocity during the burn,

$$\Delta v = v_e \ln\frac{m_0}{m_f} \Rightarrow v_e = \frac{\Delta v}{\ln\frac{m_0}{m_f}} = \frac{56\ \mathrm{m/s}}{\ln\left(\frac{27{,}320\ \mathrm{kg}}{27{,}320\ \mathrm{kg} - (1{,}521 - 862)\mathrm{kg}}\right)}$$
$$= 2{,}293\ \mathrm{m/s} \tag{4.28}$$

The specific impulse is simply the exhaust velocity divided by the gravitational constant,

$$I_{sp} = \frac{v_e}{g_0} = \frac{2{,}293\ \mathrm{m/s}}{9.80665\ \mathrm{m/s^2}} = 233.9\ \mathrm{s} \tag{4.29}$$

The total impulse is found by using the mass flow rate of the propellant, the burn time, and the exhaust velocity

$$\begin{aligned} I_t &= F t_b = \dot{m} v_e t_b \\ I_t &= \frac{\Delta m}{\Delta t} v_e t_b \\ I_t &= \frac{(1{,}521 - 862)\ \mathrm{kg}}{2\ \mathrm{s}} (2{,}294\ \mathrm{m/s})(2\ \mathrm{s}) \\ I_t &= 1{,}511\ \mathrm{kNs} \end{aligned} \tag{4.30}$$

(Continued)

Example 4.1 Spacecraft with a partial burn cycle *(Continued)*

The propellant mass fractions are calculated as follows:

$$\zeta_{p_1} = \frac{m_{p_1}}{m_0} = \frac{1{,}521\ \text{kg}}{27{,}320\ \text{kg}} \Rightarrow \zeta_{p_1} = 0.05567$$
$$\zeta_{p_2} = \frac{862\ \text{kg}}{26{,}661\ \text{kg}} \Rightarrow \zeta_{p_2} = 0.03233 \qquad (4.31)$$

4.3.3 Summary of Rocket Engine Parameters

It is often useful to have an easily accessible reference of various rocket engine performance parameters. These are tabulated in Table 4.4.

Note that although rocket engines may appear to be complex (and they are!), the design of a propulsion system is not insurmountable. As with all design exercises, the selection of a rocket engine architecture is determined by a small number of performance parameters. These are:

- Δv required for mission
- Thrust required for launch
- Propellant types and chemistry (which determine exhaust products, storability, logistics, etc.)
- Propellant density (which constrains tank volume and inert mass)
- Chamber pressure and temperature (which constrains motor material, thermal management, etc.)

Table 4.4 Rocket Engine Parameter Conversions

Thrust $T = \dot{m}c = C_T P_c A_T = C_T(c^*)\dot{m} = \dot{m} g_0 I_{sp} = \dfrac{P_c A_T g_0 I_{sp}}{c^*}$
Specific impulse (weight) $I_{sp} = \dfrac{T}{\dot{m} g_0} = \dfrac{T}{\dot{w}_p} = \dfrac{c}{g_0} = c^* \dfrac{C_T}{g_0} = \dfrac{c^*}{g_0} \cdot \dfrac{T}{P_c A_T}$
Mass flow $\dot{m} = \dfrac{T}{c} = \dfrac{T}{g_0 I_{sp}}$
Characteristic exhaust speed $c^* = \dfrac{P_c A_T}{\dot{m}} = \dfrac{T}{\dot{m} C_T} = \dfrac{g_0 I_{sp}}{C_T} = \dfrac{c}{C_T}$
Effective exhaust speed $c = \dfrac{T}{\dot{m}} = g_0 I_{sp} = c^* C_T = \dfrac{c^* T}{P_c A_T} = \dfrac{C_T P_c A_T}{\dot{m}}$
Thrust coefficient $C_T = \dfrac{T}{P_c A_T} = \dfrac{c}{c^*} = \dfrac{g_0 I_{sp}}{c^*}$

Notes: A_T = nozzle throat cross-section area
P_c = combustion chamber pressure
g_0 = Earth surface gravity acceleration = 9.80665 m/s^2 = 32.174 ft/s^2
(*) is not a multiplication sign! (c*) is *characteristic exhaust speed*, a *variable*.

4.4 Solid-Propellant Motors

Given the complexities of liquid-propellant rocket engines (discussed in greater detail in Section 4.5), it is perhaps unsurprising that a simpler option would exist. Solid-propellant motors [commonly referred to as solid rocket motors (SRMs)] certainly have a longer history than their liquid-propellant counterparts, dating back to China circa 200 BC. It therefore makes logical sense, from the perspectives of both simplicity and history, to examine SRMs first.

The solid-propellant motor utilizes a solid propellant that deflagrates (combusts subsonically) after ignition. It has several distinct advantages over its liquid-propellant counterpart: it is (relatively) inexpensive, storable, and simple in design; has high volumetric specific impulse (i.e., dense fuel); and does not require a propellant delivery system. This makes the SRM ideal for small- or medium-sized launchers, or as a reliable upper stage for orbital injection. The ease of storability of the propellant means that a solid-propellant rocket will likely need a minimum of support infrastructure relative to a liquid-propellant equivalent, simplifying the deployment strategy of an SRM. The SRM is also devoid of support equipment necessary for liquid-propellant propulsion: an SRM needs no turbopumps, plumbing, control valves, pressurant gas, or other dead weight, thus increasing its mass ratio.

However, two specific disadvantages plague SRMs, which to date have remained unresolved: the solid-propellant motor is almost guaranteed to have a lower specific impulse than a mass-comparable liquid-propellant engine (SRMs have, on average, an I_{sp} of 200–300 s), and SRMs cannot be throttled (although their thrust-time curves can be tailored, by changing the shape of their grain, to provide a varying thrust profile to match their intended mission). Hence, once an SRM is ignited, it will continue to burn (and produce thrust) until all of its fuel is consumed. This means that SRMs cannot be test-fired before their actual use; thus, their reliability must be established by analysis and similitude, which becomes quite an important consideration when designing a human-rated launch vehicle.

The solid propellant in an SRM is typically a rubbery combination of fuel, oxidizer, and a binding agent—typically aluminum, ammonium perchlorate, and a binder such as polybutadiene acrylonitrile (PBAN) are used. (Black powder is still used for smaller rockets.) Unlike for liquid propellants, the choice of propellants for an SRM is a considerably narrower field: most manufacturers will have their own optimized blends of ingredients, from which their SRMs are made. These ingredients are mixed and then cast into a pressure vessel to create the final form of the fuel. Once the fuel has solidified, it is operational.

4.4.1 Basic Configuration

From the standpoint of physics, a solid-propellant motor is identical to a liquid-propellant engine, in that both types create a hot gas via combustion

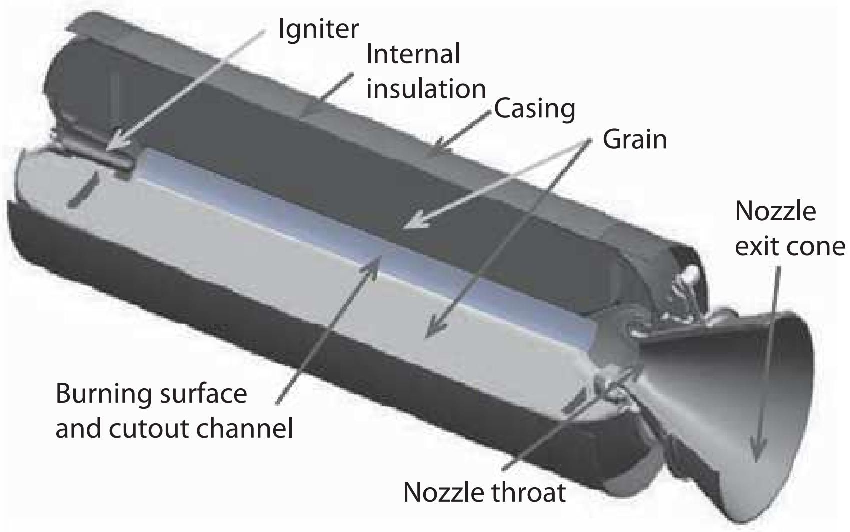

Fig. 4.9 Basic arrangement of a solid-propellant rocket motor. Source: Northrop-Grumman.

and expel it as a high-speed exhaust through a nozzle. The performance parameters given in Table 4.4 are calculated in the exact same fashion. A basic layout of a generic SRM is shown in Fig. 4.9. The requisite hot gas is produced by igniting a surface of the fuel block, known as the charge or grain. This grain is almost always bonded to the inside wall of the casing, in order to prevent the flame front from migrating along the wall of the casing, which would prematurely (and unevenly) ignite other parts of the grain and possibly cause an explosion. There is often a layer of thermal insulation to protect the inside of the motor casing from the hot burning propellant. The charge contains both fuel and oxidizer, as well as the aforementioned binder material, meaning that SRM ignition is, for the most part, a "light and leave" affair. The exhaust velocity of an SRM is not high (on the order of 2,700 m/s for the most advanced types), which contributes to its low specific impulse.

4.4.2 SRM Types and Burn Rates

There are two primary types of SRMs, as shown in Fig. 4.10: the end burner and the core burner. The *thrust period* is the primary difference between them. An end burner will have a thrust period that is low-power and relatively long (a "cigarette burn"), whereas a core burner will have a higher-thrust, shorter period (an "inside-out burn").

One of the most important parameters in the performance of an SRM is its thrust stability. For a liquid-propellant engine, it is reasonable to assume that the chamber pressure remains relatively constant throughout its operation and is determinable based on the mass flow rate of propellant through the injectors. For a solid-propellant motor, the mass flow rate is determined by the rate at which the grain is consumed; not surprisingly, this parameter is known as the *burn rate*, and for solid propellant, is itself a function of the chamber pressure.

Because of this, stable combustion in an SRM cannot be automatically assumed, because the mass flow rate of the propellant increases with chamber pressure. This is given by

$$\dot{m} = aP_c^{\beta} \tag{4.32}$$

where the parameter β (burn rate pressure exponent) controls the stability of combustion. This equation is commonly known as *de Saint Robert's law.* It has already been shown earlier in the chapter that the mass flow rate out of the combustion chamber depends on the pressure within it. Thus, for $\beta > 1$, the combustion gas from the burning grain increases with pressure at a higher rate than the rate of exhaust, which could result in an uncontrolled rise in combustion rate and chamber pressure (and, similarly, a small decrease in chamber pressure could result in a catastrophic drop in burn rate). On the other hand, for $\beta < 1$, the burning rate will always be lower than the rate of exhaust, indicating that the chamber pressure will stabilize after a perturbation. Typically, β will be between 0.4 and 0.7.

The variable a in Eq. (4.32) is known as the coefficient of pressure (or burning rate constant); together with the burn rate pressure exponent, it is part of the propellant internal ballistic characteristics. These are experimentally measured propellant characteristics that vary among propellants. Equation (4.32) describes the *nonerosive burn rate*, and it should thus stand to reason that if nonerosive burning exists, so too does erosive burning. The total burn rate for an SRM, then, is a summation of these two burn rates. For a solid-propellant motor, the conditions at the upper and lower extremes of the charge are different: at the top of the charge, the newly formed exhaust gas is fairly stagnant, whereas at the bottom of

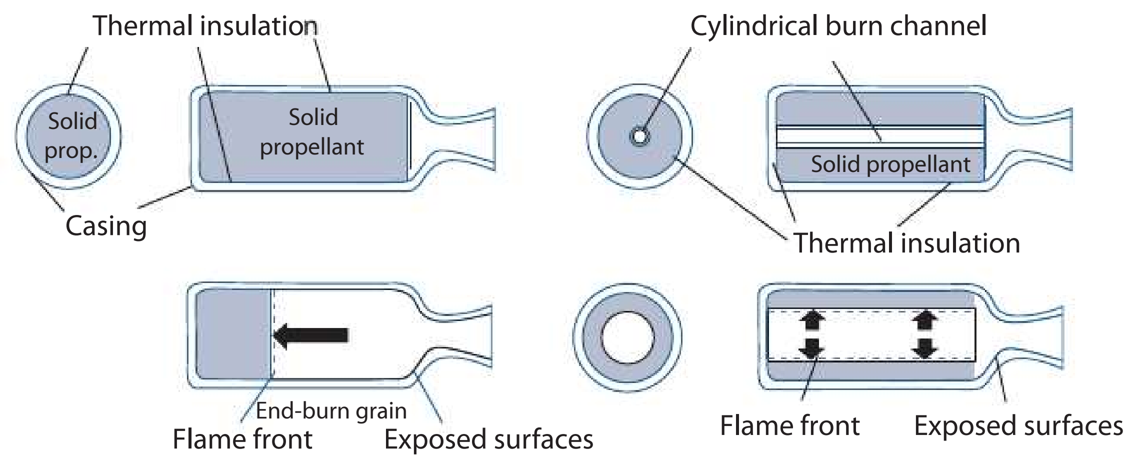

Fig. 4.10 Two primary types of SRMs: left: end burner; right: core burner.

the charge the gas is moving very fast. Near the nozzle, this results in a high recession (the rate at which the propellant is consumed and moves away from the nozzle), which if left unchecked can cause a burn-through of the nozzle or a failure of the casing before the upper portion of the propellant is consumed. This phenomenon can be mitigated by having an increasing cross-sectional area near the nozzle. For a constant flow rate, an increase in cross-sectional area causes a decrease in velocity, and thus erosive burning can be forestalled.

4.4.3 Thrust Profile and Grain Shape

The rate at which the grain is combusted directly influences the chamber pressure, and hence the thrust. The chamber pressure depends on two parameters: the area of the burning surface and the recession rate of the grain. The mass flow rate of propellant depends on the volume of grain consumed per second. Although SRMs cannot be throttled, their grain can be shaped to produce different levels of thrust for different periods of time. This is accomplished by inserting mandrels into the motor casing during the solid propellant casting process (Fig. 4.11), which produce cutouts in the cross-section of the grain. This changes the total burn area, which in turn produces varying *thrust profiles*, some examples of which are shown in Fig. 4.12.

The mass flow rate of an SRM is entirely dependent on the burn area A_b, the burn rate b_r, and the density of the propellant ρ

$$\dot{m} = \rho A_b b_r \tag{4.33}$$

Thus, the relationship between mass flow rate (and hence thrust) and burn area is easily seen.

Fig. 4.11 Mandrels used during casting process of solid propellant.

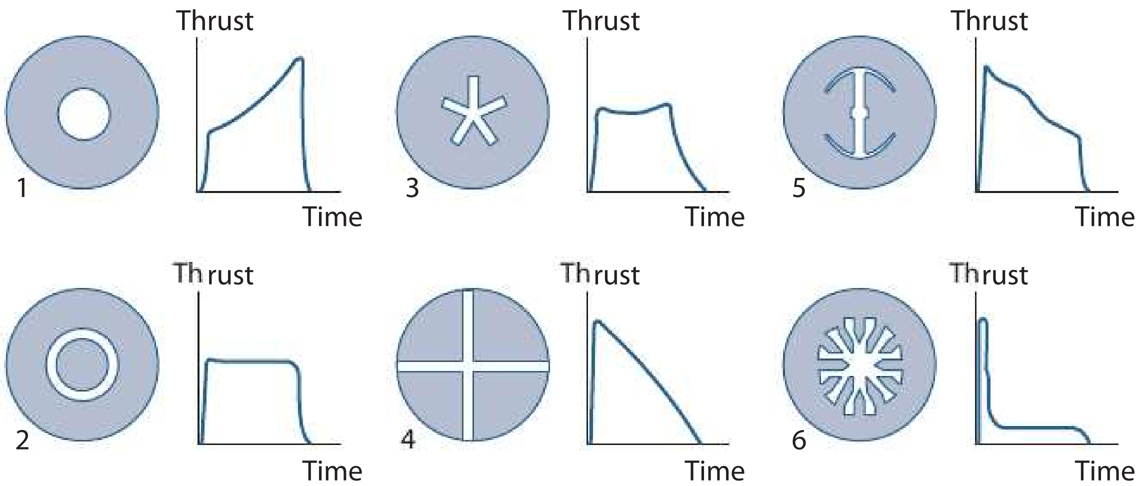

Fig. 4.12 Examples of grain shapes and accompanying thrust profiles. Source: http://www.braeunig.us/

The simplest thrust profile is that of the end burner, whose grain is illustrated on the left side of Fig. 4.10; this type of grain will produce a nearly constant thrust level until all of the propellant is consumed. For this profile, the burning area is limited to the cross-sectional area of the casing, and the burning rim of the grain will be in contact with the inner wall of the casing; because active cooling of the casing wall is not an option with solid-propellant motors, this type of grain is typically only used for short, low-thrust periods.

The hollow cylindrical grain (#1 in Fig. 4.12) begins burning along the inner surface of the cutout, which presents the advantage of the unburned grain insulating the motor casing from the flame front. The burn area of the grain can also be much larger than for a solid cylindrical grain, improving thrust performance. A grain with a cylindrical cutout will produce thrust levels that increase with time, which may be handy for certain applications (e.g., a solid-propellant missile can be fired from a wingtip without forcing the nose of the aircraft to yaw off-target). For a constant thrust, a secondary grain cylinder or a cog-shaped cutout (#2 and #3 in Fig. 4.12, respectively) can be used. Other grain shapes will produce different profiles. The resourceful propulsion engineer is in no way restricted to using one grain pattern throughout the entirety of the SRM. Mixing grain profiles, especially in large boosters, is quite common. For instance, the initial segments of an SRM can have a star-shaped profile (#6 in Fig. 4.12) to maximize thrust during liftoff while reducing thrust as the launch vehicle accelerates through max-q, and then have later segments feature a double-cylinder grain profile. This allows the thrust of the SRM to be tuned according to the mission requirements and the capabilities of a given launch vehicle.

The burn rate, and thus the thrust profile, of solid-propellant motors is significantly affected by ambient temperature. This is because the rate at which the grain is consumed is dependent upon the rate at which the grain is heated. This, in turn, depends on the rate of heat supplied by combustion and the temperature of the grain itself: if the grain is very cold, more heat must be supplied before the grain can combust. The grain itself is very heavy, and is therefore a good insulator. Variations in burn rate by a factor of two due to variations in temperature between –15°C and 20°C have been reported [7]. This will affect the thrust profile of the SRM, which could actually cause the mission to fail if the motors do not produce sufficient thrust.

4.4.4 SRM Propellant Additives

In modern propellants, metallic powders are often added to aid in combustion and increase the combustion temperature, thereby increasing the energy released during launch. Aluminum is commonly used, and because the resultant aluminum oxide found in the exhaust stream is *refractory* (i.e., retains its strength at elevated temperatures), it remains solid as it is being ejected from the motor. Solid particles in the exhaust stream are detrimental to thrust, because they travel slower than the surrounding high-velocity gas (due to the higher molecular weight of the particulates) and are efficient radiators of heat, thereby reducing the overall energy of the stream.

For most heterogeneous solid propellants, the oxidizer is the primary constituent (by mass), and the binder is the fuel. Aluminum may also be present at 16–18% (by mass), along with other chemicals intended to improve the safety and/or performance of the motor. Carbon compounds are often present, which will render the propellant opaque to infrared radiation, so that propellant "upstream" of the flame front will not be ignited by the burning surface. Plasticizers increase the plasticity of the grain to improve the molding and extruding characteristics of the fuel. Up to 1% iron oxide is sometimes added in order to smooth the combustion process.

In addition to improving the performance of the motor, several other additives can also be added to increase the stability of the fuel, which affects its storage qualities and mechanical strength. The mechanical strength of the fuel is a very important property: the fuel must be resistant to cracking during handling, because cracks will increase the total surface area of the fuel exposed to a flame front. This can lead to uneven burning, or even an explosion. The fuel not undergoing combustion must also withstand the launch loads, including accelerations of 10 g or more, without failing.

4.4.5 SRM Exhaust Toxicity

When firing a rocket engine near the ground, the majority of the exhaust is dispersed across a wide area surrounding the launch site. Unlike liquid-propellant engines, the combustion products of SRMs usually contain particulate matter, as well as approximately 12% hydrogen chloride by mass (which the chemically minded reader will recognize as a gas that forms hydrochloric acid when in contact with atmospheric humidity). Other products of combustion can include aluminum oxide, carbon monoxide, carbon dioxide, water vapor, nitrogen, and hydrogen. The combined molecular weight of the gaseous exhaust products is approximately 25 g/mol. By comparison, the molecular weight of aluminum oxide is 102 g/mol. Note that this two-phase flow is actually more beneficial than the alternative: if the aluminum oxide was also in a gaseous state, the molecular weight of the exhaust would be very high, producing a slow-moving exhaust stream that would degrade the performance of the motor.

Because of exhaust toxicity, it is therefore important that the SRM exhaust stream be channeled via ductwork as appropriate. Obviously, this is not possible once the rocket is in flight, and atmospheric dispersal must be relied upon. Most solid-propellant launch sites will require a thorough cleaning after launch, which can take several days.

4.5 Liquid-Propellant Engines

A liquid-propellant rocket engine is, simply, a rocket engine that uses liquid propellants. These engines may be *monopropellant*, *bipropellant*, or of the more exotic *tripropellant* variety, depending on the number of propellants the engine consumes to produce thrust. Although any number of propellants is theoretically possible, the vast majority of liquid engines in use today will be of the mono- or bipropellant variety. These propellants are typically fed to the thrust chamber using pumps or pressurant gas, where they are then mixed and combusted to produce thrust. A monopropellant is a propellant that releases energy through exothermic chemical *decomposition*, usually through the use of a catalyst. This is different from bipropellants, which usually release energy via chemical *reaction* between the fuel and oxidizer. Monopropellants may be multiple substances or a single substance with the desired properties, such as hydrogen peroxide or hydrazine.

Literally thousands of combinations of liquid propellants have been tried over the course of history, but in the end only three practical types of liquid propellant are used: cryogenic, semicryogenic, and hypergolic. A cryogenic propellant, as the name implies, is one that requires very low temperatures in order to liquefy (e.g., for liquid oxygen, this is around −193°C or 90 K). A semicryogenic fuel (e.g., kerolox, a mixture of kerosene fuel and liquid oxygen oxidizer) is one in which at least one component is storable (i.e., liquid at ambient temperature). Hypergolic propellants are storable chemicals that auto-ignite upon contact with one another.

The primary advantage of a liquid engine over a solid motor is that a liquid engine will typically have a much higher specific impulse than a solid motor, with the attendant increases in overall vehicle performance. Also, many liquid engines can be throttled by changing the propellant mass flow rate, which provides designers more flexibility in how a launch vehicle (or spacecraft) delivers the thrust necessary for its mission. Liquid propellants typically have a higher energy density than their solid-propellant counterparts, which means that the volume of the propellant tanks may be relatively low; the structural weight of the propellant tanks can also be reduced by using pumps and compressors to deliver the propellants to the combustion chamber, which allows the propellants to be kept under low pressure to minimize the tank wall thickness. This arrangement improves the mass ratio for the rocket. Alternatively, an inert gas (e.g., helium) at high pressure can be used in lieu of pumps to force the propellants into the combustion chamber; these engines will have a lower mass ratio, but are usually more reliable [8]. If high-pressure gas is used in lieu of pumps, the propellant storage tanks must sustain the pressure provided by the high-pressure gas, resulting in more wall thickness and more massive tanks. The common ways of delivering propellant to the engine, pump-fed and pressure-fed, are shown in Fig. 4.13.

The primary disadvantages of liquid engines arise due to two factors: propellant storability and all-up mass of the propellant subsystems.

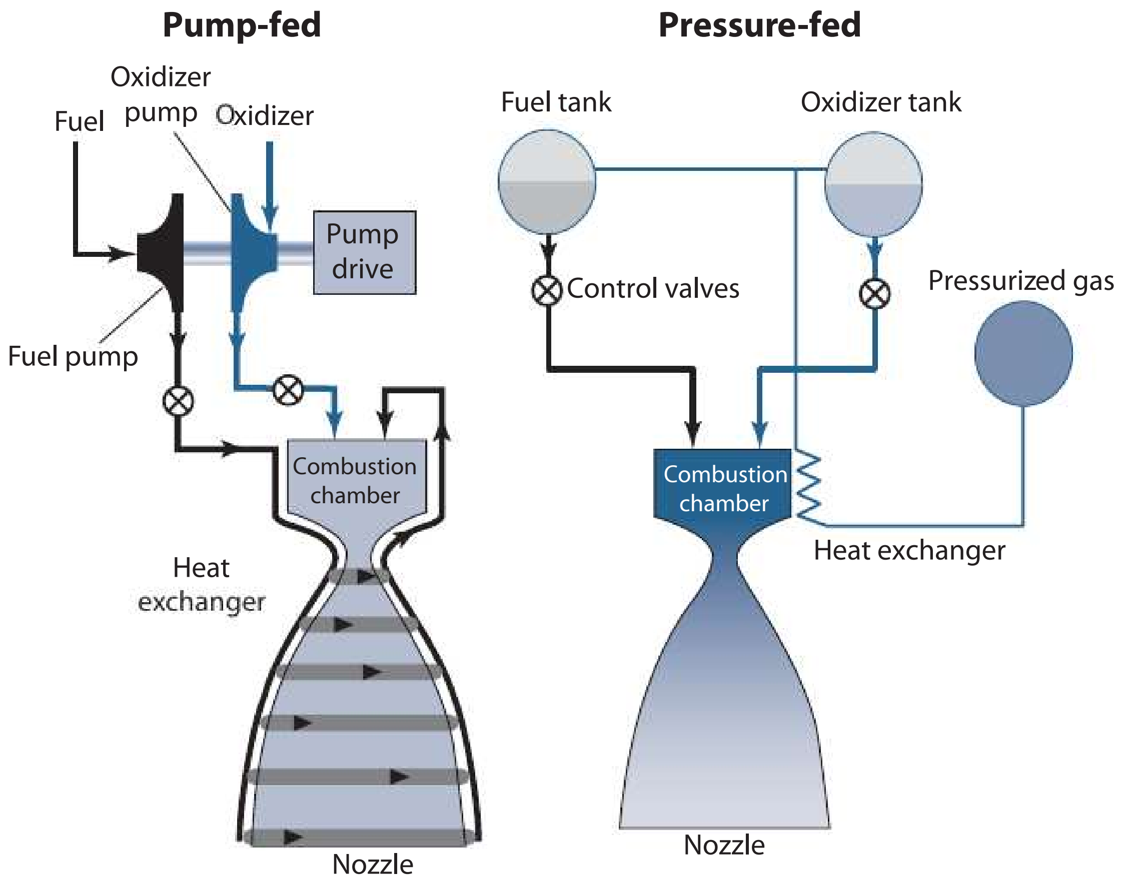

Fig. 4.13 In a liquid-propellant engine, propellants are delivered to the combustion chamber either using pumps or pressure. A pump-fed engine uses a mechanical pump to raise pressure, while a pressure-fed engine uses a high-pressure reservoir. Valves are opened or shut to start or stop flow. Propellant may be used to cool nozzle walls, known as *regenerative cooling*. An ignition source is also needed, except for hypergolics.

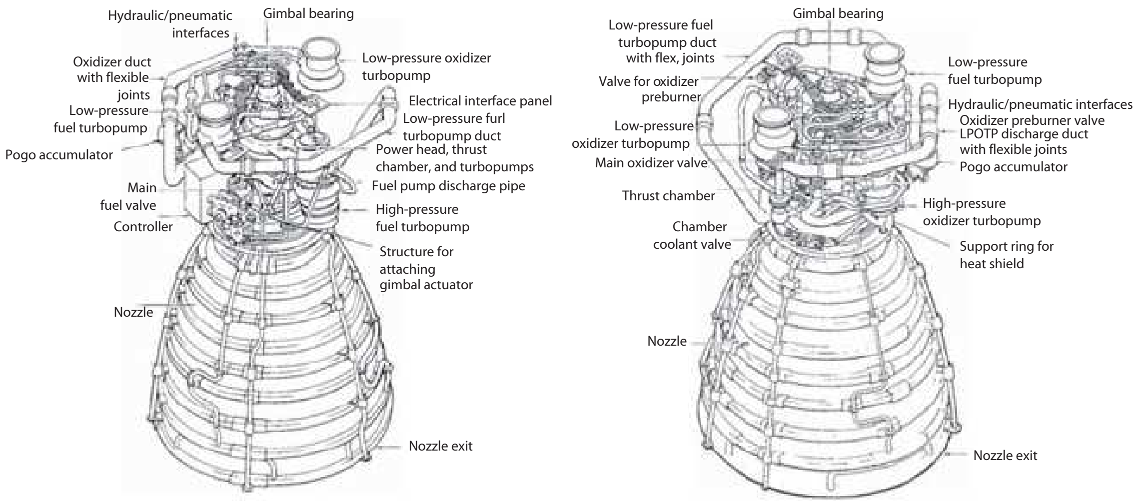

Fig. 4.14 Two views of the Space Shuttle main engine. Source: [8].

Cryogenic propellants must be kept cold to be usable, which in turn requires insulation and venting. Propellant boil-off is a very real issue, which is governed by the amount of thermal leakage of the tanks as well as the percentage of propellants present (partially filled tanks experience faster boil-off). By the square-cube law, the smaller the tank, the faster the boil-off. Boil-off is also dependent upon temperature: the low temperatures required to store liquid hydrogen (–253°C or 20 K) mean it can experience a boil-off of 13–17% per day, whereas the higher temperature of liquid oxygen can limit the boil-off to 2.2–2.6% of tank capacity per day [10]. This can become a very real concern when a launch must be continually delayed. By contrast, hypergolic propellants are typically easily storable, at the cost of requiring very specific handling procedures (and the associated constraints on the vehicle lifecycle), due to the fact that many hypergolic propellants have a high toxicity and carcinogenicity. The liquid engine architecture also requires that propellants be transported from one location to another (e.g., from the propellant tanks to the combustion chamber) via pumps or pressurant gas, which increases the inert weight of the propulsion system. Illustrations of liquid-propellant engines, such as the Space Shuttle main engine shown in Fig. 4.14, offer a hint at just how complex these engine architectures can become.

The mass of the propellant subsystems must also be carefully taken into account during the design phase. Although the propellant mass is an important parameter, equally important is the mass of the propellant tanks: they must not only be strong enough to store the propellants and survive the launch loads, but also be sufficiently lightweight to maintain a favorable mass ratio. With cryogenic propellants, this problem is compounded, because the tanks must also be insulated. Additional tank mass is required for pressure-fed systems. Properties of common liquid propellants are given in Tables 4.5 and 4.6.

Table 4.5 Properties of Common Cryogenic Propellants

Propellant	Boiling Point, K	Mass, g/mol	Formula	I_{sp} with LOx	O/F, kg/kg$_{LOx}$	Density, kg/m^3
LOx	90	32	O_2	–	–	1,141
RP-1	460+	175	$CH_{1.97}$	250	0.43	810–1,020
LH_2	20.4	2.01	H_2	360+	0.15	71
Methane	112	16.04	CH_4	268	0.41	424
Propane	231	44.1	C_3H_8	260	0.34	733

Table 4.6 Properties of Common Storable and Hypergolic Propellants

Propellant	Melting Point, K	Mass, g/mol	Formula	Density, kg/m^3
Dinitrogen tetroxide (DNTO or NTO)	261.5	92.02	N_2O_4	1,450
Monomethyl hydrazine (MMH)	220.7	46.08	CH_3NHNH_2	874
Hydrazine	274.5	32.05	N_2H_4	1,005
Unsymmetrical dimethyl hydrazine	216	60.1	$(CH_3)_2NNH_2$	791
Aerozine 50 (50% Hydrazine – 50% UDMH)	266.15	92.14	50% N_2H_4, 50% $(CH_3)_2NNH_2$	1,450
Ethanol	159	46.07	C_2H_5OH	789.3
Methanol	175.6	32.04	CH_3OH	791.4
HTP (high-test peroxide)	272.2	34.0	H_2O_2	1,443
Nitromethane	244.2	61.04	CH_3NO_2	1,137

4.6 Examples of Rocket Engine Performance

4.6.1 SRM Performance

The theoretical performance of solid-propellant motors using common oxidizer–fuel combinations is given in Table 4.7. Note that these figures are for a chamber pressure of 1,000 psia (6,895 kPa) at sea level, with a perfectly expanded nozzle and frozen combustion. For comparison, the performance characteristics of several large SRMs, including sea-level I_{sp}

Table 4.7 Theoretical SRM Performance

Oxidizer	Fuel	ρ, g/cm^3	T, K	c^*, m/s	MW, g/mol	I_{sp}, s
NH_4NO_3	11% binder, 7% additives	1.51	1,282	1,209	20.1	192
NH_4ClO_4	18% polymer, 4–20% Al	1.69	2,816	1,590	25.0	262
NH_4ClO_4	12% binder, 20% Al	1.74	3,371	1,577	29.3	266

Table 4.8 Performance of Sample Large SRMs

Motor	Gross Mass, kg	Empty Mass, kg	T, kN	I_{sp}, s	t_b, s
Space Shuttle SRB	590,000	88,000	11,520	235	123
Delta II GEM-46	19,327	2,282	628	273	75
Atlas V	40,824	4,000	1,270	245	94
Delta IV GEM-60	33,978	3,849	827	243	90
Ariane V EAP	278,330	38,200	6,470	250	130
Minuteman M-55	23,077	2,292	792	237	60

and burn time t_b, are given in Table 4.8. Note that for large SRMs, mass ratios of 8–10 are not uncommon, reinforcing the idea that rocket motors must maximize the total propellant mass carried for each pound of inert structure.

The performance figures for several "kick" motors is given in Table 4.9. These are more commonly referred to as *apogee kick motors (AKMs)*, and they are regularly used on spacecraft intended for geostationary orbit. This allows a launch vehicle to place a spacecraft in an elliptical orbit with a nonzero inclination, at which point the spacecraft must generate its own thrust to provide the Δv required to reach geostationary orbit. An AKM thus "kicks" the speed of the spacecraft up to to the necessary orbital speed.

4.6.2 Liquid Engine Performance

The theoretical performance of some common liquid fuels and oxidizers is listed in Table 4.10. Note that any fuel listed in Table 4.10 with a percent

Table 4.9 Performance of Several Kick Motors

Motor	Total Impulse, N	Gross Mass, kg	ζ_p	$\overline{T}$, N	I_{sp}, s
STAR-13B	1.16E5	47	0.88	7,015	286
STAR-30BP	1.46E6	543	0.94	26,511	292
STAR-30C	1.65E6	628	0.95	31,760	285
STAR-30E	1.78E6	667	0.94	35,185	289
STAR-37F	3.02E6	1,149	0.94	44,086	291
STAR-48A	6.78E6	2,559	0.95	79,623	284
IUS SRM-2	8.11E6	2,995	0.91	80,157	304
LEASAT PKM	9.26E6	3,658	0.91	157,356	285
IUS SRM-1	2.81E7	10,374	0.94	198,435	296

Table 4.10 Theoretical Performance of Liquid-Propellant Engines

Oxidizer	Fuel	Mass f	Vol. f	S.G.	T_C, K	c^*, m/s	MW, kg/kmol	I_{sp}, s
LOx	75% ethanol	1.30	0.98	1.00	2,904	1,641	23.4	267
		1.43	1.08	1.01	2,957	1,670	24.1	279
	Hydrazine	0.74	0.66	1.06	3,027	1,871	18.3	301
		0.90	0.80	1.07	3,127	1,992	19.3	313
	Hydrogen	3.40	0.21	0.26	2,416	2,428	8.9	388
		4.02	0.25	0.28	2,724	2,432	10.0	391
	RP-1	2.24	1.59	1.01	3,282	1,774	21.9	286
		2.56	1.82	1.02	3,399	1,804	23.3	300
	UDMH	1.39	0.96	0.96	3,171	1,835	19.8	295
		1.65	1.14	0.96	3,321	1,864	21.3	310
DNTO	Hydrazine	1.08	0.75	1.20	2,857	1,765	19.5	283
		1.34	0.93	1.22	2,977	1,782	20.9	292
	Aerozine 50	1.62	1.02	1.18	2,957	1,731	21.0	278
		2.00	1.24	1.21	3,088	1,745	22.6	288

sign refer to fuels by mass percent composition; also, the fuel "Aerozine 50" refers to a fuel that is equal parts UDMH and hydrazine. The two sets of values listed in Table 4.10 are for frozen (upper) or shifting (lower) equilibrium at an assumed chamber pressure of 1,000 psia (6,895 kPa) and a sea-level ambient pressure (14.7 psia, 101.4 kPa) at the nozzle exit. These figures also assume optimum expansion ratio, adiabatic combustion, and isentropic expansion. Specific gravities are provided at their boiling point or at 68° F/1 atm (20° C/101.4 kPa), whichever is lower.

A commonly used figure of merit for liquid-propellant engines is their *thrust-to-weight ratio*, or $\frac{T}{W_{\text{engine}}}$, a dimensionless ratio that describes how efficient an engine is by itself. The engine thrust-to-weight ratio is useful because the engine(s) is(are) one of the largest contributors to a rocket's inert or dry weight as may be seen in Fig. 8.28 of Chapter 8. This *engine* T/W_{engine} ratio should not be confused with the *vehicle's* T/W ratio, which is the ratio of thrust to *loaded* weight.

It is instructive to compare the theories presented so far with real-world examples of liquid-propellant engines. Perhaps the most famous liquid-propellant engine is the Rocketdyne F-1, which powered the first stage of the Saturn V launch vehicle. Its performance specifications are given in Table 4.11, and the engine is shown in Fig. 4.15. In the table, "SA5xx" refers to the xx-th mission of the Saturn V LV.

The specifications for the Rocketdyne J-2, which powered second stage of the Saturn IB and the second and third stages of the Saturn V, are given in

Table 4.11 Rocketdyne F-1 Specifications

	Vehicle Effectivity	
	SA501-SA503	SA504 and Subsequent
Thrust (sea level), MN	6.672	6.77
Thrust duration, s	150	165
I_{sp}, s	260	263
Engine dry mass, kg	8,353	8,391
Engine mass (burnout), kg	9,115	9,153
Exit/throat area ratio	16	16
Propellants	LOx/RP-1	LOx/RP-1
f	2.27% $\pm$ 2%	2.27% $\pm$ 2%
T/W_{engine}	74.6	75.4

Source: NASA.

Fig. 4.15 Rocketdyne F-1 engine on display at Kennedy Space Center. Source: NASA.

Table 4.12 Rocketdyne J-2 Specifications

	Vehicle Effectivity		
	SA201-SA203	SA204-SA207 SA501-SA502	SA208 and Subsequent SA504 and Subsequent
Thrust (altitude), kN	889.6	1,000.9	1,023
Thrust duration, s	500	500	500
I_{sp}, s	418	419	421
Engine dry mass, kg	1,579	1,579	1,584
Engine mass (burnout), kg	1,637	1,637	1,642
Exit/throat area ratio	27.5	27.5	27.5
Propellants	LOx/LH_2	LOx/LH_2	LOx/LH_2
f	$5.00 \pm 2\%$	$5.50 \pm 2\%$	$5.50 \pm 2\%$
T/W_{engine}	55.4	62.3	63.5

Source: NASA.

Table 4.12, and the engine is shown in Fig. 4.16. In the table, "SA2xx" refers to the xx-th mission of the Saturn IB LV, and "SA5xx" refers to the xx-th mission of the Saturn V LV.

The Rocketdyne RS-68 is used as the first-stage engine for the Delta IV launch vehicle, and currently is the largest hydrogen-fueled rocket engine in the world. Unlike many other liquid-propellant engines, the RS-68 has an ablative nozzle lining; this nozzle lining burns away during flight to dissipate heat. Although this solution is heavier than a conventional tube-wall regeneratively-cooled nozzle, it reduces part count and is easier to manufacture, thus lowering the engine's cost. The specifications for the RS-68 are given in Table 4.13, and the engine is shown in Fig. 4.17.

Note that the RS-68's T/W_{engine} is significantly lower than the previous engines, probably due to the extra weight of the ablative nozzle lining.

A summary of performance characteristics of common liquid-propellant rocket engines, compiled from various sources, is given in Table 4.14.

A more modern engine, the SpaceX Merlin 1D, is shown in Fig. 4.18. This engine runs on RP-1 and LOx but shows very high performance: each engine produces 845 kN of thrust, with an astonishing $T/W_{engine} = 179.8$. This engine is said to have the highest value of the T/W_{engine} parameter.

4.7 Rocket Engine Power Cycles

It may correctly be surmised from Table 4.14 that the power cycle will have an impact on an engine's performance, either directly (via combustion) or indirectly (via feed systems and support hardware). The term *power cycle* is a useful method for categorizing rocket engines, and refers to how power is

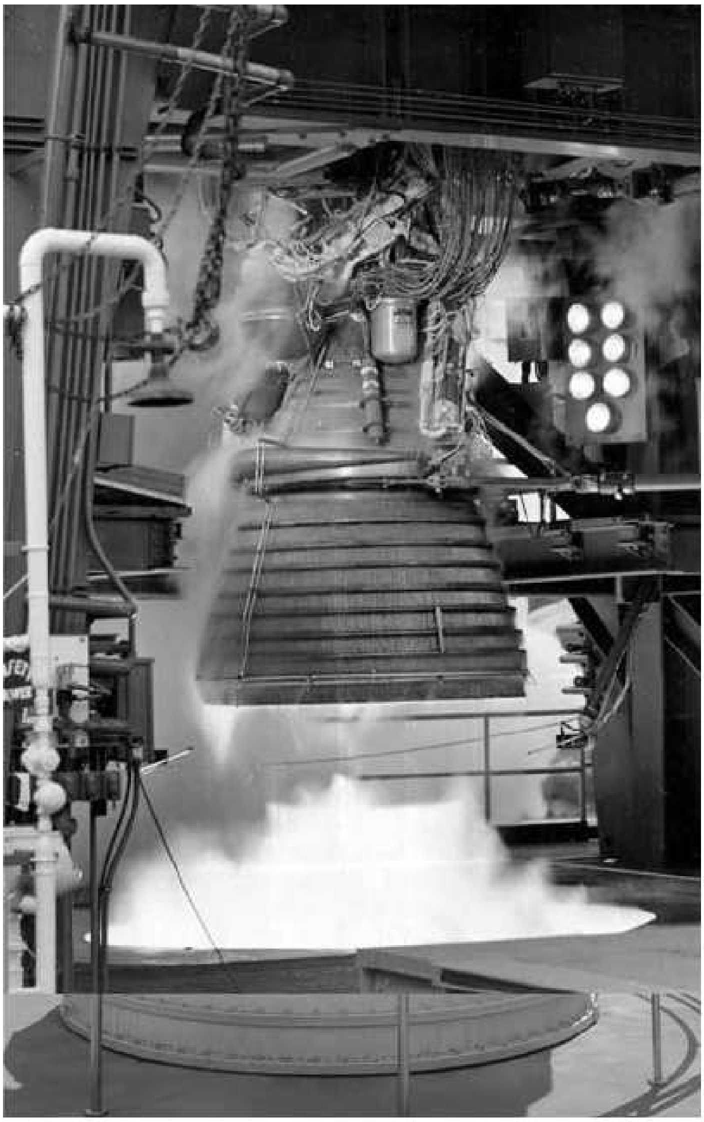

Fig. 4.16 Rocketdyne J-2 during test firing. Source: NASA.

Table 4.13 Rocketdyne RS-68 Specifications

	Vehicle Effectivity	
	RS-68	RS-68A
Thrust (sea level), kN	2,936	3,136
I_{sp}, s	410	412
Engine dry mass, kg	6,604	6,745
Exit/throat area ratio	21.5	21.5
Propellants	LOx/LH_2	LOx/LH_2
T/W_{engine}	45.3	47.4

Source: Aerojet Rocketdyne.

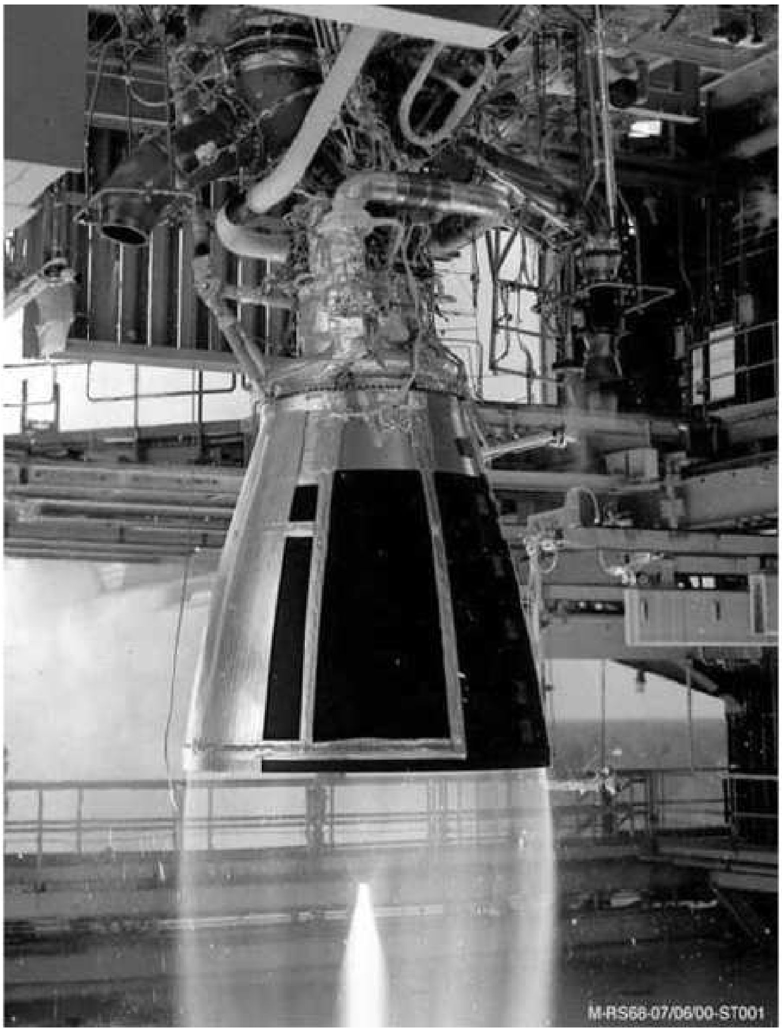

Fig. 4.17 Rocketdyne RS-68 during test firing. Source: NASA.

derived to drive pumps that feed propellants to the combustion chamber(s). This control and feeding of propellants to the combustion chamber is accomplished through the use of various plumbing, pump, valve, and control components known as the powerhead. Generally speaking, the most common types of power cycles are as follows:

- Gas generator cycle
- Staged combustion cycle
- Expander cycle
- Open expander cycle
- Pressure-fed cycle
- Electric pump-fed

Each power cycle is discussed briefly in the following sections.

Before we look at the different power cycles, let's consider the turbopump, a mechanical pump used to force propellants into a combustion chamber. A generic turbopump is shown in Fig. 4.19. In the figure, an

Table 4.14 Performance Characteristics of Selected Liquid-propellant Engines

Engine	Thrust, kN		I_{sp}, s		P_c, MPa	f	A/A^*	Geometry		Ox/Fuel	Cycle
	SL	Vac	SL	Vac				L, m	D, m		
MA-5A Sust	269	378	220	309	5.07	2.27	25:1	2.46	1.22	LOx/RP-1	Gas gen
MA-5A Boost	1,910	2,104	265	296	4.96	2.25	8:1	2.57	1.22	LOx/RP-1	Gas gen
RS-27A	890	1,054	255	302	4.83	2.25	12:1	3.78	1.44	LOx/RP-1	Gas gen
RD-170	7,255	1,909	307	337	24.13	2.6	36:1	4.01	1.45	LOx/RP-1	Staged
RD-180	3,827	4,150	311	338	25.51	2.72	36.8:1	3.58	1.45	LOx/RP-1	Staged
Merlin 1V	N/A	411	N/A	342	N/A	N/A	N/A	N/A	N/A	LOx/RP-1	Gas gen
Merlin 1A	319	N/A	270	300	N/A	N/A	N/A	N/A	N/A	LOx/RP-1	Gas Gen
Merlin 1C	614.7	N/A	275	304	N/A	N/A	N/A	N/A	N/A	LOx/RP-1	Gas gen
LR87-AJ-11	1,984	2,353	254	302	5.70	2	15:1	3.84	1.50	N_2O_4/A-50	Gas gen
LR91-AJ-11	N/A	445	N/A	314	5.70	1.86	49.2:1	2.79	1.63	N_2O_4/A-50	Gas gen
RD-253	1,472	1,637	285	316	14.70	2.67	26.2:1	2.72	1.43	N_2O_4/UDMH	Staged
RD-0210	N/A	588	N/A	327	14.69	2.65	78.2:1	2.30	1.46	N_2O_4/UDMH	Staged
HM-60	885	1,140	334	431	11.00	5.3	45:1	2.87	1.75	LOx/LH_2	Gas gen
RL10A-4-1	N/A	99.2	N/A	451	4.21	5.5	84:1	1.78	1.17	LOx/LH_2	Expander
RL10B-2	N/A	110.3	N/A	467	4.44	6.0	285:1	3.05	2.14	LOx/LH_2	Expander
RS-68	2,891	N/A	365	410	9.72	6.0	12.5:1	N/A	N/A	LOx/LH_2	Gas gen
SSME 109%	1,818	2,279	380	453	22.48	6.0	77.5:1	4.27	2.44	LOx/LH_2	Staged

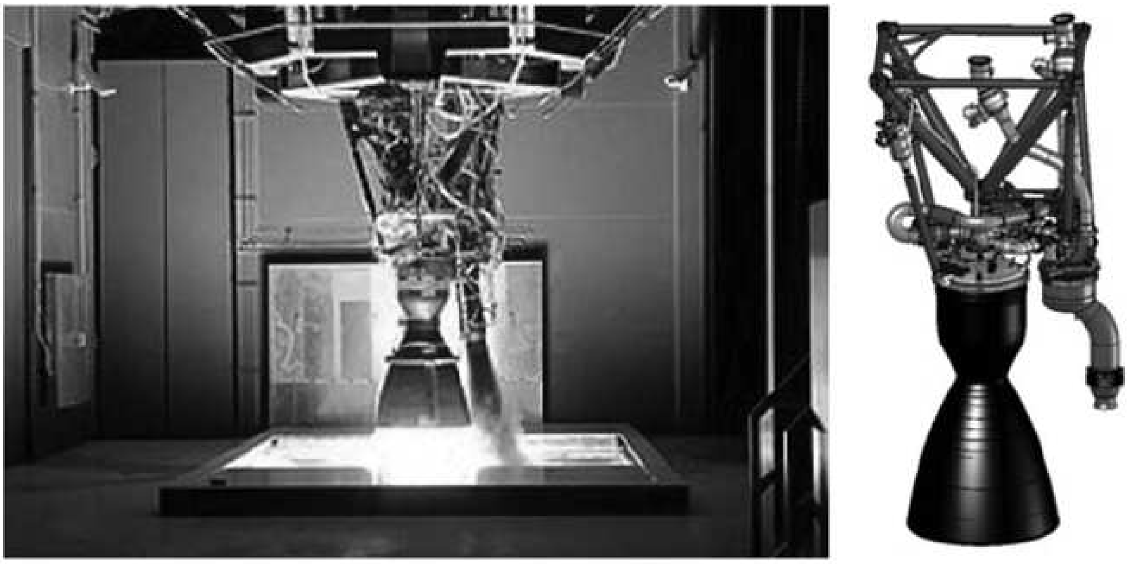

Fig. 4.18 SpaceX's Merlin 1D produces 845 kN of thrust, and has a very high $T/W_{engine} = 179.8$. Courtesy: SpaceX.

impeller (upper right) is driven to a very high rotational speed by a set of turbine blades driven by high-pressure gas (lower right). The impeller increases the pressure of the incoming propellant enough to be able to force it into the high-pressure combustion chamber. The engine's *cycle* determines where the high-pressure turbine drive gas comes from.

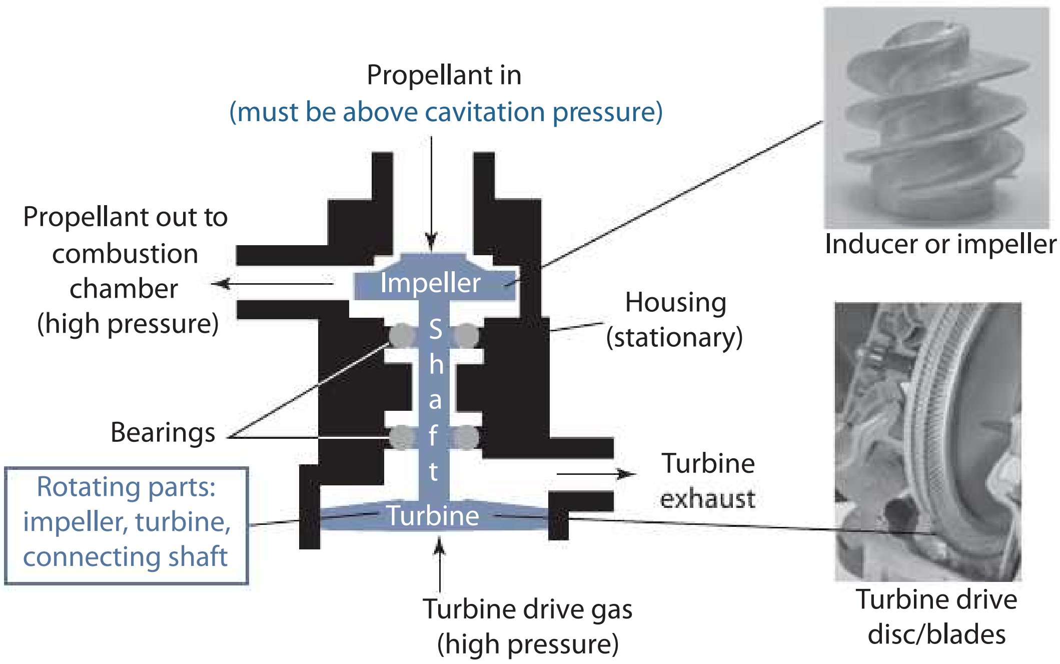

Fig. 4.19 A turbopump uses a turbine to drive the impeller which sucks in propellants and raises their pressure above that of the combustion chamber pressure. Courtesy: NASA blog.

4.7.1 Gas Generator Cycle

The gas generator cycle is shown schematically in Fig. 4.20. In this power cycle, a small amount (approximately 3–7%) of fuel and oxidizer is diverted from the main propellant flow into a preburner, which powers a turbine that drives the fuel and oxidizer pumps, which in turn feed propellants into the combustion chamber. A gas generator engine will typically burn propellants at a suboptimal mixture ratio (the engine will run oxidizer-rich) in order to keep the turbine blade temperature low. Unused exhaust from the preburner is either dumped or sent into the nozzle. Because there will always be some amount of propellant exhausted from the power turbine, the gas generator cycle is also referred to as an *open cycle.*

The key advantage of the gas generator cycle is that the power turbine does not need to inject the turbopump exhaust against the backpressure of combustion, simplifying the design of the engine's plumbing and turbine, which may result in a lighter and less expensive engine. The disadvantage of this power cycle is, of course, the lost efficiency stemming from the diverted propellant used to drive the power turbine; this results in gas

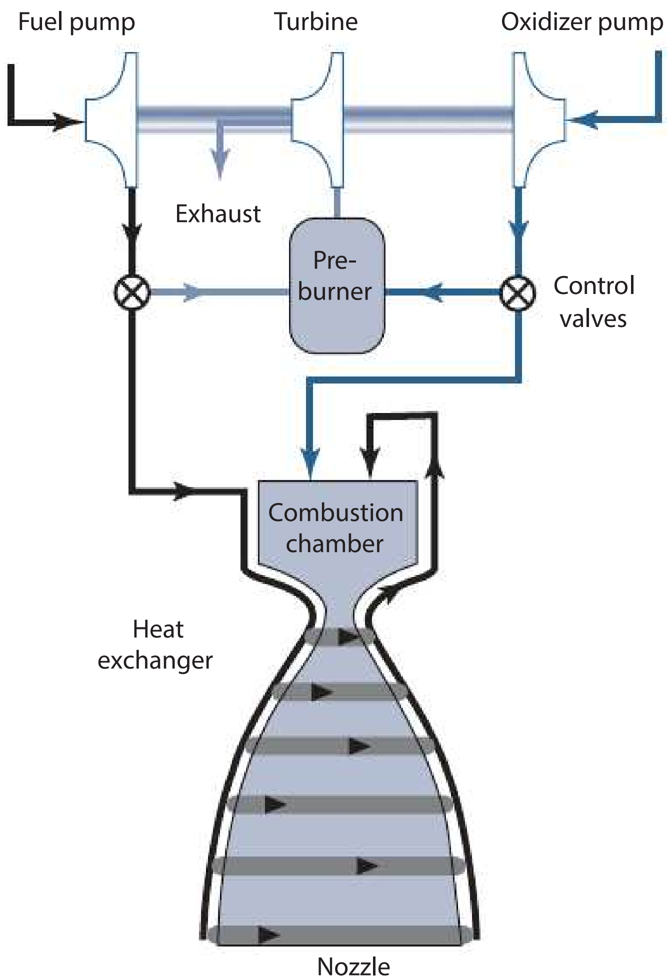

Fig. 4.20 The gas generator power cycle.

generator engines operating at a lower specific impulse than engines utilizing other power cycles. The RS-68 engine is an example of the gas generator cycle.

4.7.2 Staged Combustion Cycle

The staged combustion cycle, also known as a *topping cycle*, is one where the propellants are combusted in stages. This power cycle is often used for high-power applications, such as the RD-180 or NK-33 engines. A preburner generates the working fluid for a power turbine (which drives the propellant pumps) as either a fuel- or oxidizer-rich gas mixture. Unlike the gas generator cycle, the staged combustion cycle injects the exhausted gas mixture from the power turbine into the combustion chamber, where the gas mixture burns again along with the second propellant. The staged combustion cycle is shown schematically in Fig. 4.21; as is usually the case, one or more propellants can be used as a coolant, simultaneously cooling the engine and preheating the propellant.

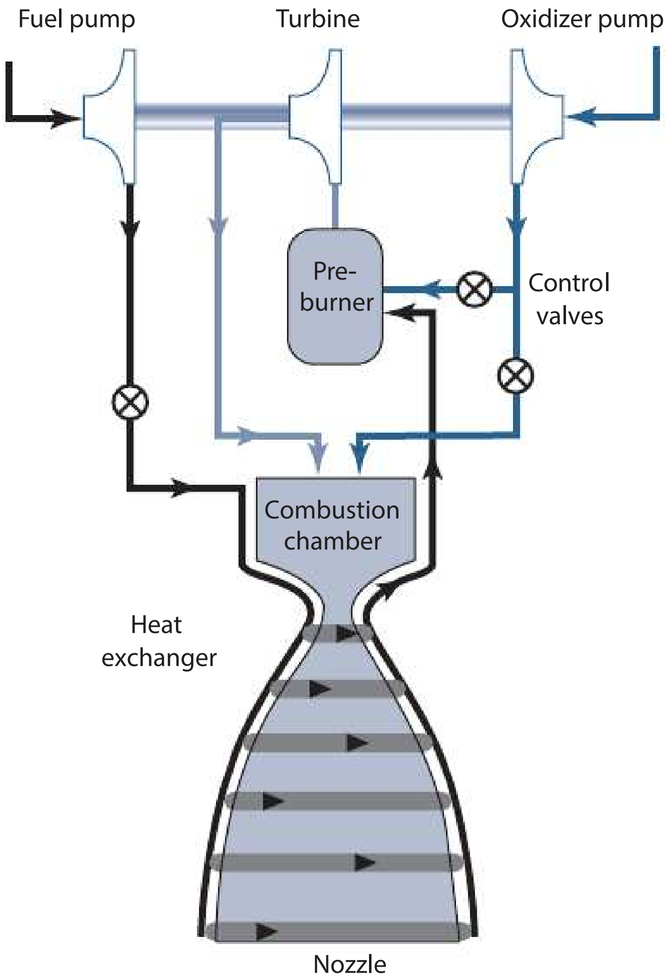

Fig. 4.21 A fuel-rich staged combustion power cycle. (Fuel injection into combustion chamber omitted for simplicity.)

The primary advantage of this "closed" type of power cycle is obvious: all of the propellant is routed through the combustion chamber. Staged combustion engines typically use high-power turbopumps, resulting in high chamber pressures and allowing the use of large nozzle area ratios to improve the low-altitude performance of the engine. These advantages come at a cost, however, and staged combustion cycles usually require exotic materials for plumbing and valves to carry the hot gas mixture, along with complicated control systems. Engines using oxygen-rich staged combustion (such as the NK-33), in particular, require advanced materials due to the corrosive oxidizer-rich gas mixture; by contrast, the primary concern of a fuel-rich staged combustion engine is the use of a noncoking fuel, such as liquid hydrogen.

A variant of the staged combustion cycle is known as the full flow staged combustion cycle (FFSC; see Fig. 4.22). An FFSC uses both an oxidizer- and a

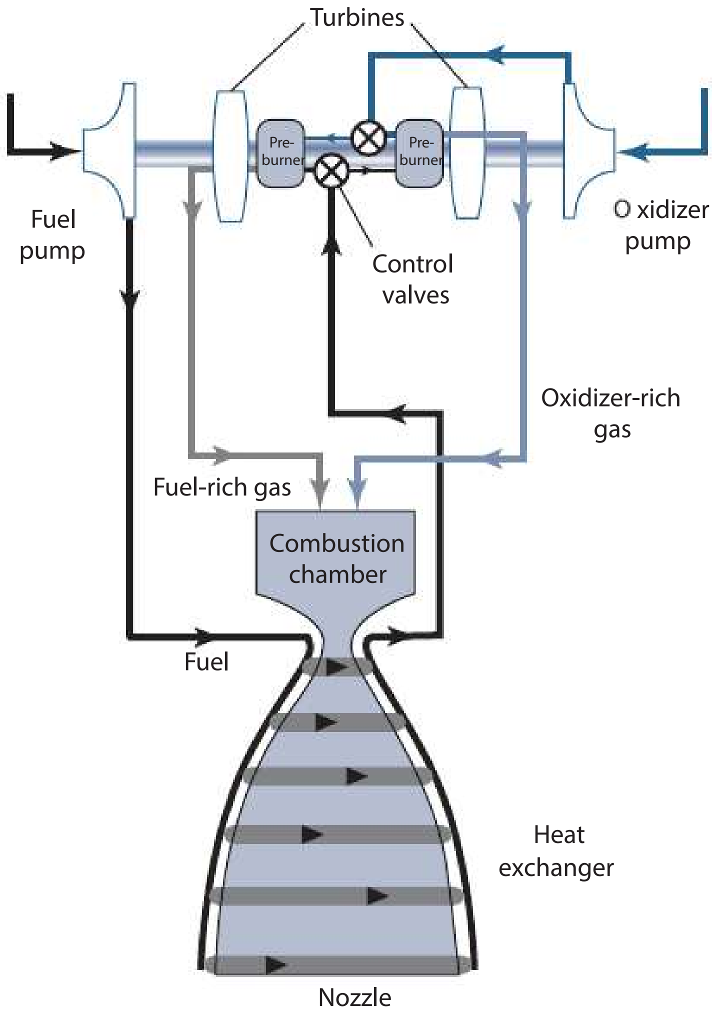

Fig. 4.22 The full-flow staged combustion cycle. Fuel and oxidizer are burned together in two separate pre-burners: one preburner drives the fuel turbine; the other drives the oxidizer turbine. Exhausts from both turbopumps are injected into the combustion chamber for highest efficiency. Example: SpaceX Raptor engine. (Fuel and oxidizer injection into combustion chamber omitted for simplicity.)

fuel-rich preburner, which permits the power turbine to be powered by both propellants. (This arrangement also results in full gasification of both propellants, leading FFSC engines to occasionally be referred to as "gas-gas" engines.)

Fuel & oxidizer are burned in two separate pre-burners in 'stages'; one is fuel-rich, one is oxidizer -rich. The resulting gases are used to drive turbopumps: the fuel-rich pre-burner drives the fuel turbopump; the oxidizer-rich pre-burner drives LOx turbopump. The turbopump exhausts are then injected into the combustion chamber for maximum efficiency.

This cycle also allows a unique advantage over regular staged combustion: an FFSC engine has its fuel and oxidizer pumps driven by two separate power turbines, thus permitting independent control over the flow of both propellants. Also, both turbines will usually operate at lower temperatures and pressures in this configuration, which has a direct impact on both engine life and reliability. The SpaceX Raptor engine is an example of the full-flow staged combustion cycle.

4.7.3 Expander Cycle

An expander cycle is similar to a staged combustion cycle, with the key difference being that an expander cycle does not use a preburner. The heat in the combustion chamber cooling jacket vaporizes the fuel, which then passes through the power turbine and injects into the combustion chamber along with the oxidizer. Expander cycles work well with propellants that have a low boiling point and are easily vaporized, such as liquid hydrogen and methane. The expander cycle is shown schematically in Fig. 4.23.

Although the propellants will burn at or near the optimal mixture ratio in the combustion chamber (and no flow is dumped overboard), the expander cycle is limited by the amount of heat able to be transferred to the fuel in the cooling jacket, which in turn limits the available power to the turbine. Therefore, the expander cycle is usually best employed in small and midsize engines such as the RL-10, RL-60, LE-5A/B, and Vinci engine.

This thrust limitation in conventional closed expander cycle engines is due to the square-cube law: as the nozzle size increases (with increasing thrust levels), the surface area from whence heat is extracted to vaporize the fuel increases as the square of the nozzle radius; however, the volume of fuel that must be vaporized increases as the cube of the nozzle radius. There exists, therefore, a practical limit (of about 300 kN of thrust) beyond which a conventional closed expander cycle (such as that shown in Fig. 4.23) will not be able to vaporize sufficient fuel to drive the power turbine.

To bypass this limitation, several expander cycle engines utilize a dual-expander cycle (i.e., both the fuel and oxidizer are vaporized in their cooling jackets and are then used to drive their respective, independent power turbines), a closed split-expander cycle (i.e., propellants are fed

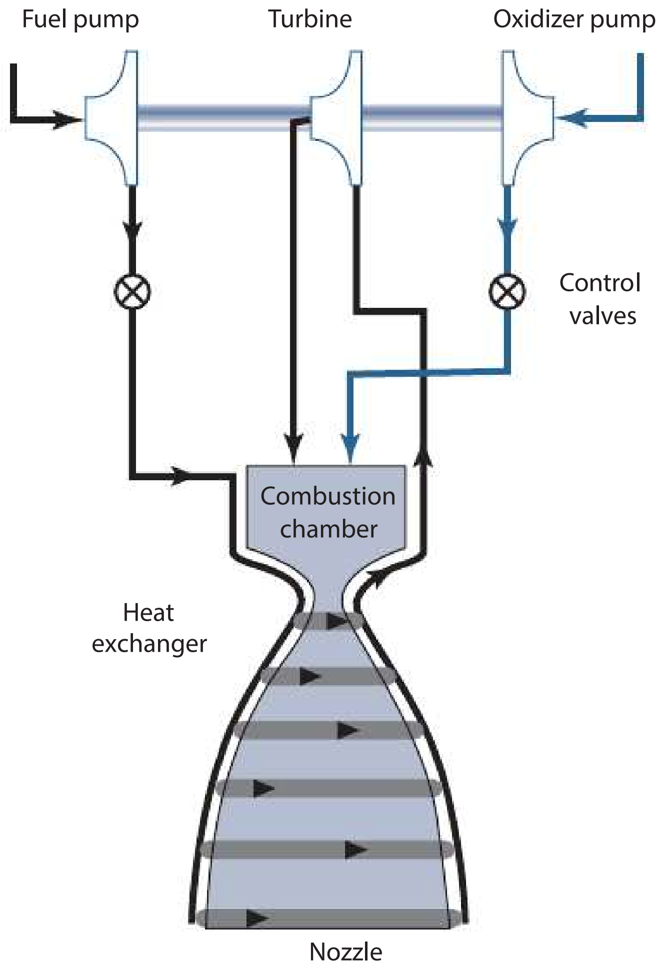

Fig. 4.23 The closed expander cycle. (Fuel injection into combustion chamber omitted for simplicity.)

through a secondary pump stage prior to injection into the combustion chamber, in order to recover some of the pressure losses induced by circulating through the cooling jacket), and even gas generator–augmented expander cycles (different from a conventional gas generator cycle in that, in this case, the combustion products from the gas generator are pumped through a heat exchanger and then exhausted overboard, rather than directly driving the power turbine).

A notable variation on the expander cycle is the open expander cycle (or "bleed" expander), wherein only a small portion of the fuel is used to drive the power turbine, and the working fluid is exhausted overboard (to ambient pressure) after passing through the turbine. This increases the turbine pressure ratio, increasing the power output of the engine via higher chamber pressures than are typically available with the closed expander cycle at the cost of decreased efficiency (lower specific impulse) due to the overboard flow. This is shown schematically in Fig. 4.24. The expander cycle has a number of advantages over other configurations. First and foremost, the operating temperature of the turbine in an expander cycle is very low relative

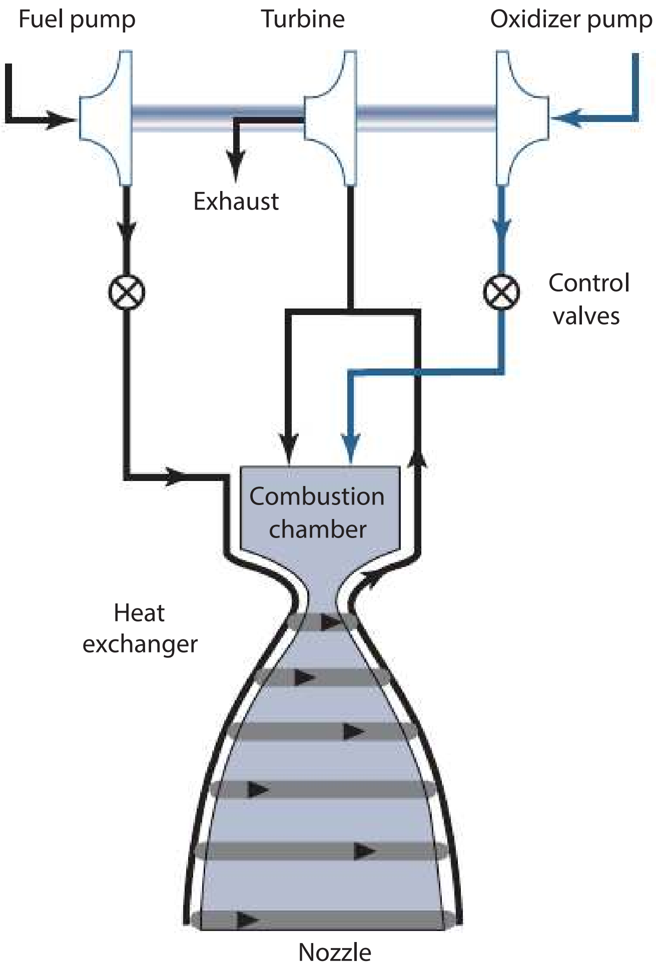

Fig. 4.24 The open expander cycle.

to a gas generator or staged combustion cycle; after the gasification of the fuel, the working fluid is usually near room temperature and will do little damage to the turbine. Secondly, an expander cycle can be more tolerant of fuel contamination due to the wide channels used in the nozzle cooling jacket; by contrast, gas generator cycles are very sensitive to blockage, and even a small hot spot can cause an "unscheduled rapid disassembly" of the engine. This also leads to the characteristic of inherent safety: because the nozzle is used as a heat exchanger, an expander cycle engine is immune to unintended feedback problems caused by malfunctioning valves.

4.7.4 Electric Pump-Fed Cycle

Note that it is not necessarily a requirement to use a preburner to drive a power turbine, which in turn drives the propellant pumps. The propellant pumps can instead be driven via electric motors, which are then powered by an onboard generator or battery. This arrangement is known as an electric pump-fed cycle. (The word *electric* is specifically used to differentiate this configuration from others that use turbine-driven pumps, such as the gas generator cycle and staged combustion cycle.) Typically, a electric motor of this type can increase propellant pressure up to 1,500 to 2,900 psi at the combustion chamber. Additionally, electric pumps can have operating efficiencies on the order of 95%, as opposed to approximately 50% for the power turbine on a typical gas generator cycle.

The main advantage of this cycle is its potential simplicity: a great deal of the complexity arising from the various plumbing, valves, turbines, pumps, preburners, feed lines, return lines, and so forth inherent in many other cycles can simply be done away with. To appreciate the magnitude of this idea of simplified propellant feeds, consider a conventional peroxide pump-fed alcolox (LOx/alcohol) rocket engine, as shown in Fig. 4.25. The attraction of an electric pump-fed system becomes readily apparent.

It should be noted that the simplicity of an electric pump-fed configuration is only a *potential* advantage: an electric pump-fed architecture will, by its very nature, require some manner of electric power to operate. Because propellant pumps are typically high-powered turbomachinery, it stands to reason that the electric pumps will need a significant battery bank, generator, or some other electric source to be effective, which may increase the inert mass of the launch vehicle. The Electron two-stage launch vehicle (developed by New Zealand Rocket Lab), designed to loft CubeSats for commercial customers, is one of the few well-funded, large-scale projects using electric pump-fed engines. The Rutherford engine powering the Electron is the first flight-ready engine to use the electric pump-fed cycle, and can provide 5,000 lb_f of (vacuum) thrust at a specific impulse of 327 s. Interestingly, the Electron jettisons several battery modules during launch, as they are expended. The electric pump-fed cycle is shown schematically in Fig. 4.26.

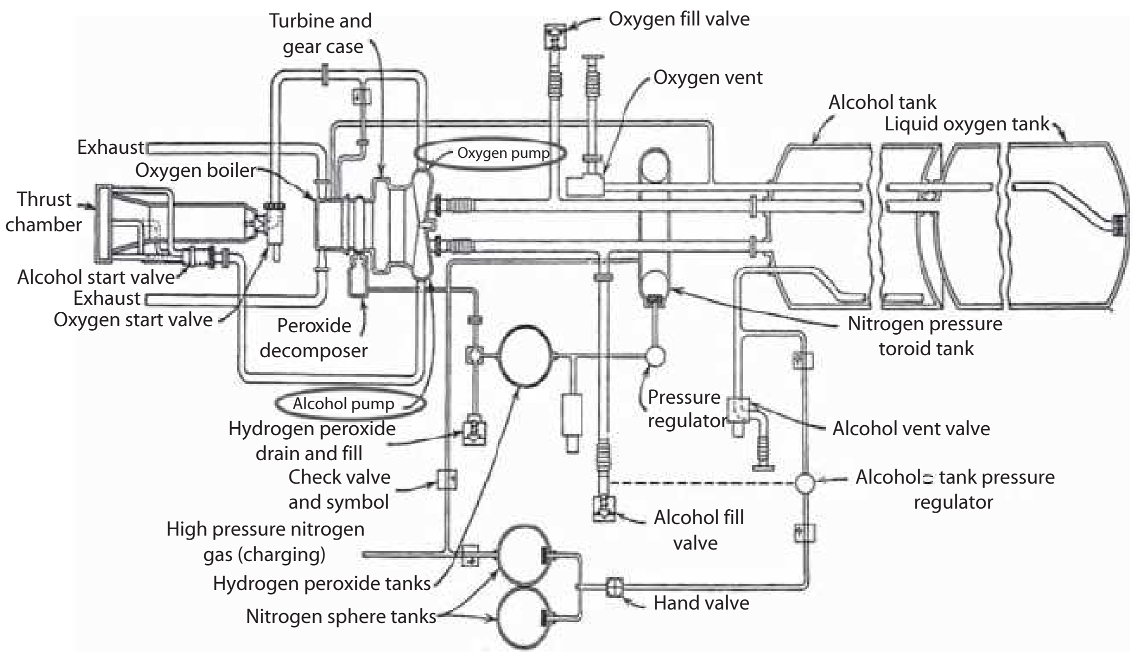

Fig. 4.25 Schematic of a LOx/alcohol engine. Source: Ordway et al. [9].

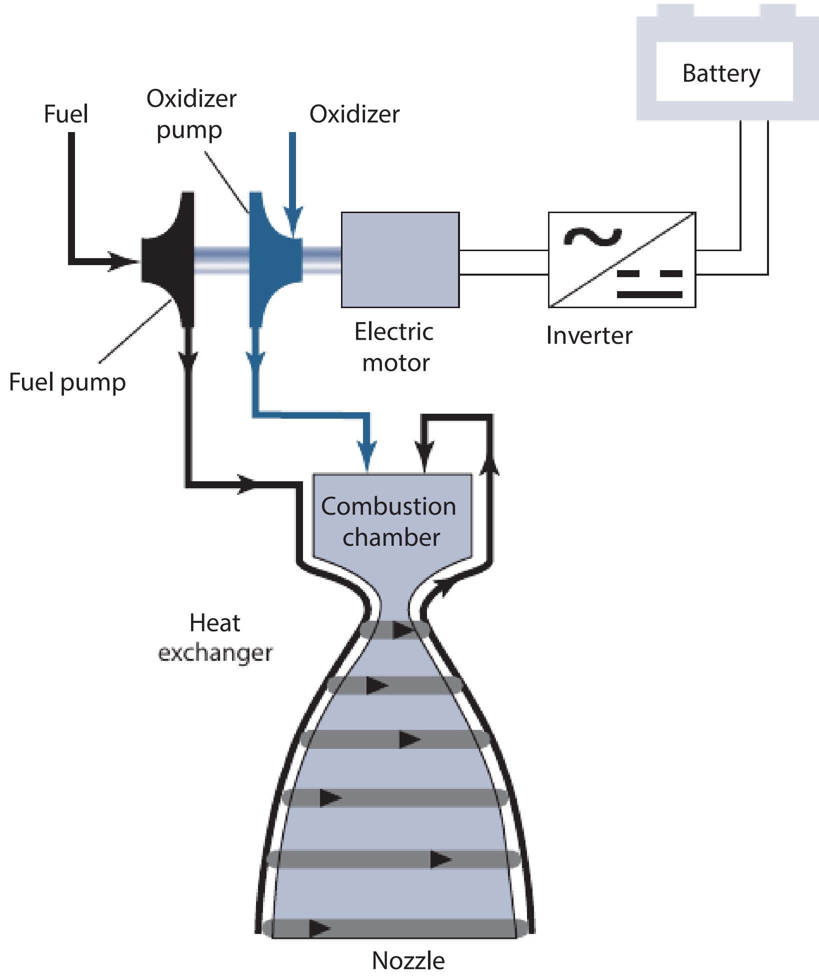

Fig. 4.26 The electric pump-fed combustion cycle.

4.7.5 Pressure-Fed Cycle

The pressure-fed cycle, like that found in the second stage of the Delta II, is the simplest arrangement possible. In lieu of pumps and turbines, the propellants are forced into the combustion chamber purely by the pressure within the propellant tanks. The tank pressure is provided by a pressurant gas, usually helium. The pressurant gas is usually stored in a separate tank known as a "bottle" and may be a composite overwrap pressure vessel (COPV), which is pressurized to approximately 350 bar (on the order of 5,000 psi or 34.5 MPa); the pressurant gas is then plumbed to the propellant tanks through a regulator and safety release valve. This configuration limits the chamber pressure, because to maintain steady propellant flow and consistent combustion, the tank pressures must exceed the chamber pressure; a higher chamber pressure would thus necessitate higher tank pressures, which would require thick tank walls and increase the inert mass of the launch vehicle (which would then result in decreased performance or reduced payload capacity). The pressure-fed cycle is shown schematically in Fig. 4.27.

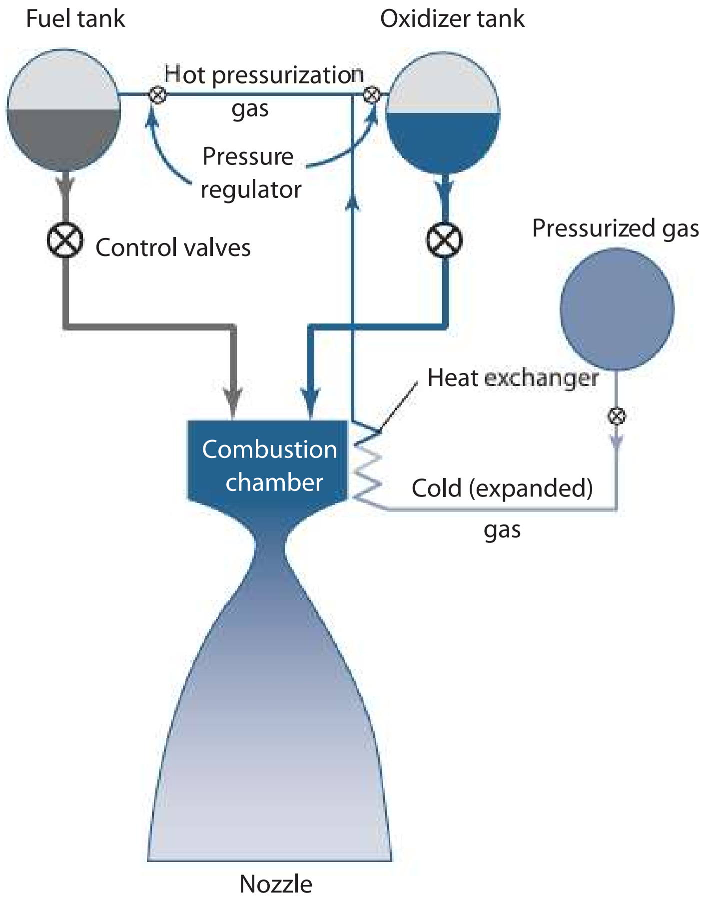

Fig. 4.27 The pressure-fed combustion cycle.

The pressure-fed cycle may not produce the highest thrust levels, but it *is* reliable due to the greatly reduced parts count and low inherent complexity. An example of this simplicity is seen in Fig. 4.28. One specific type of pressure-fed system, known as a *blowdown* system, can have as few as seven components (in addition to the required plumbing): the engine, two propellant tanks, two fill valves for the pressurant gas, and two fill valves for the propellants. This creates a unique design problem: during extended burns, excessive cooling of the pressurant gas (due to adiabatic expansion) must be avoided. The pressurant gas will not necessarily liquefy, but the excessive cold could freeze the propellants, reduce tank pressure, and damage components that are not rated for cryogenic use.

Due to the simplicity and reliability of pressure-fed engines they are used almost exclusively by spacecraft attitude control systems, maneuvering thrusters, and landers. The reaction control system (RCS) and orbital maneuvering system (OMS) of the Space Shuttle orbiter were pressure-fed designs, as were the RCS and service propulsion system engines on the Apollo command/service module. Other examples include the SuperDraco and Draco RCS engines on the Dragon V2; the RCS, ascent, and descent engines on the Apollo lunar module; the Armadillo Aerospace Pixel

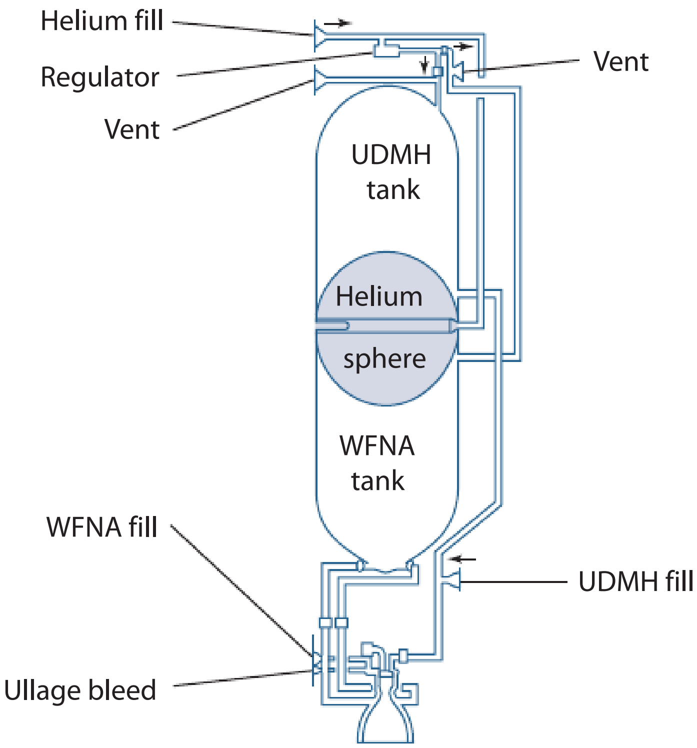

Fig. 4.28 Hypergolic pressure-fed engine. Source: Riley and Sailor [11]. WFNA = white fuming nitric acid.

vehicle designed to compete in the 2006 Lunar Lander Challenge; and the NASA Project Morpheus and Mighty Eagle prototype landers.

Pressure-fed engines have also found their way onto launch vehicles, especially as upper-stage engines. For instance, the Aerojet AJ10 and TRW TR-201 have both been used on Delta launch vehicles; the SpaceX Kestrel engine has been used on the Falcon 1 upper stage and the CONAE Tronador II upper stage. Pressure-fed systems have even been used on rocket-powered aircraft, such as the XCOR EZ-Rocket.

It is apparent that the selection of power cycle is not an arbitrary decision. As shown in Fig. 4.29, the amount of launch vehicle all-up mass devoted to structural elements is strongly tied to not only the propellant type, but also the power cycle used. Although the data in Fig. 4.29 represent trends rather than absolutes, this is a useful figure for the early stages of the design process.

4.8 Aerospike Engines

With a conventional, fixed nozzle, the expansion of exhaust gases is ideal at only a single ambient pressure. This means that the rocket engine will be operating in a nonoptimal state at all but one specific altitude. Turning a conventional nozzle "inside out," however, would allow the exhaust gas to be ideally expanded at all altitudes. This type of engine known as an *aerospike*, was to be explored in the X-33 VentureStar. A typical aerospike, known as a linear aerospike, is shown in Fig. 4.30.

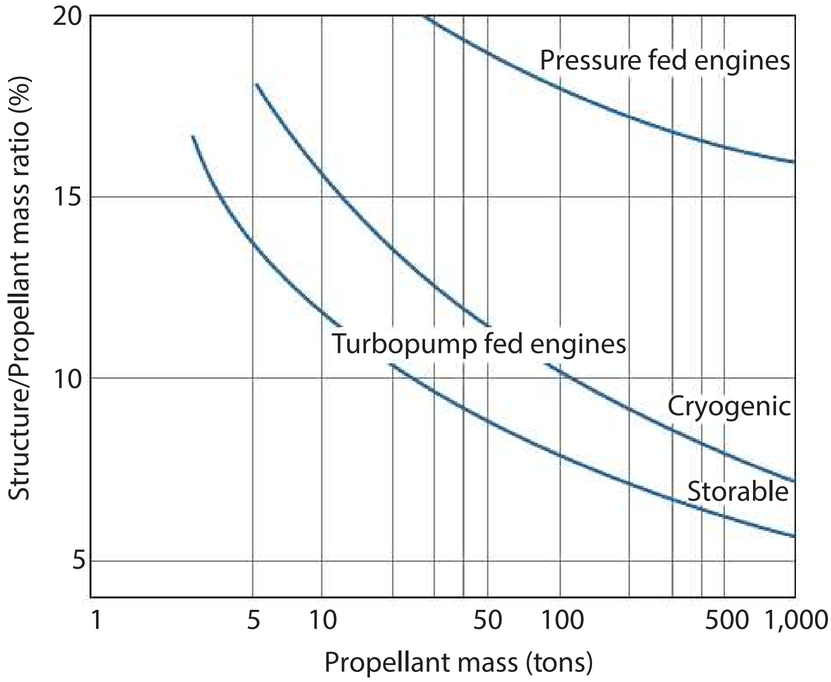

Fig. 4.29 Mass ratio of common power cycles.

The effects of altitude on nozzle performance are shown pictorially in Fig. 4.31. From Fig. 4.31a, it is readily seen that as a launch vehicle ascends, the exhaust plume will expand past the boundaries of the nozzle and assume an increasingly random motion, degrading performance. An aerospike avoids this by directing exhaust along the contour of a wedge-shaped protrusion (the "spike" portion of the aerospike name), which

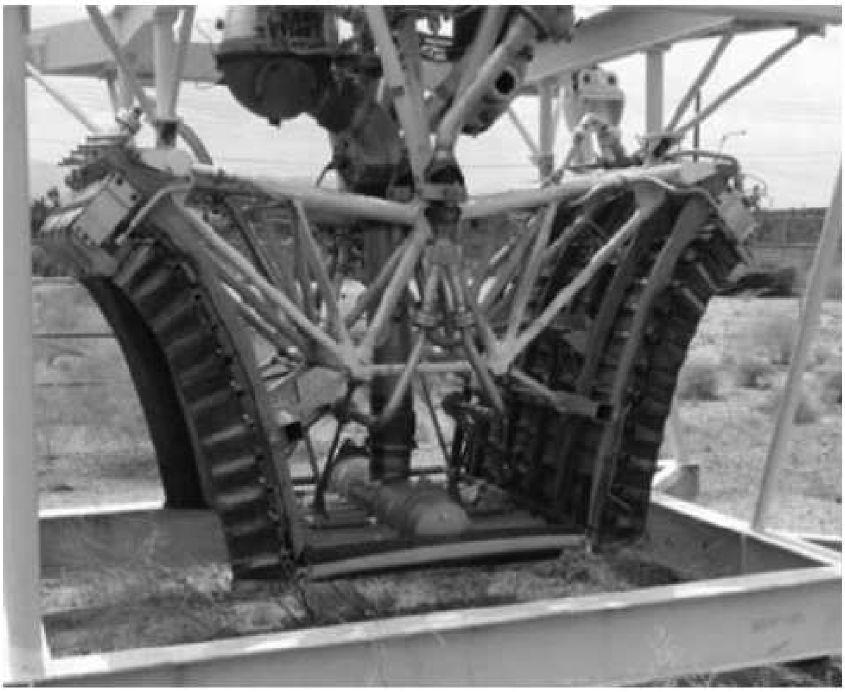

Fig. 4.30 Linear aerospike engine.

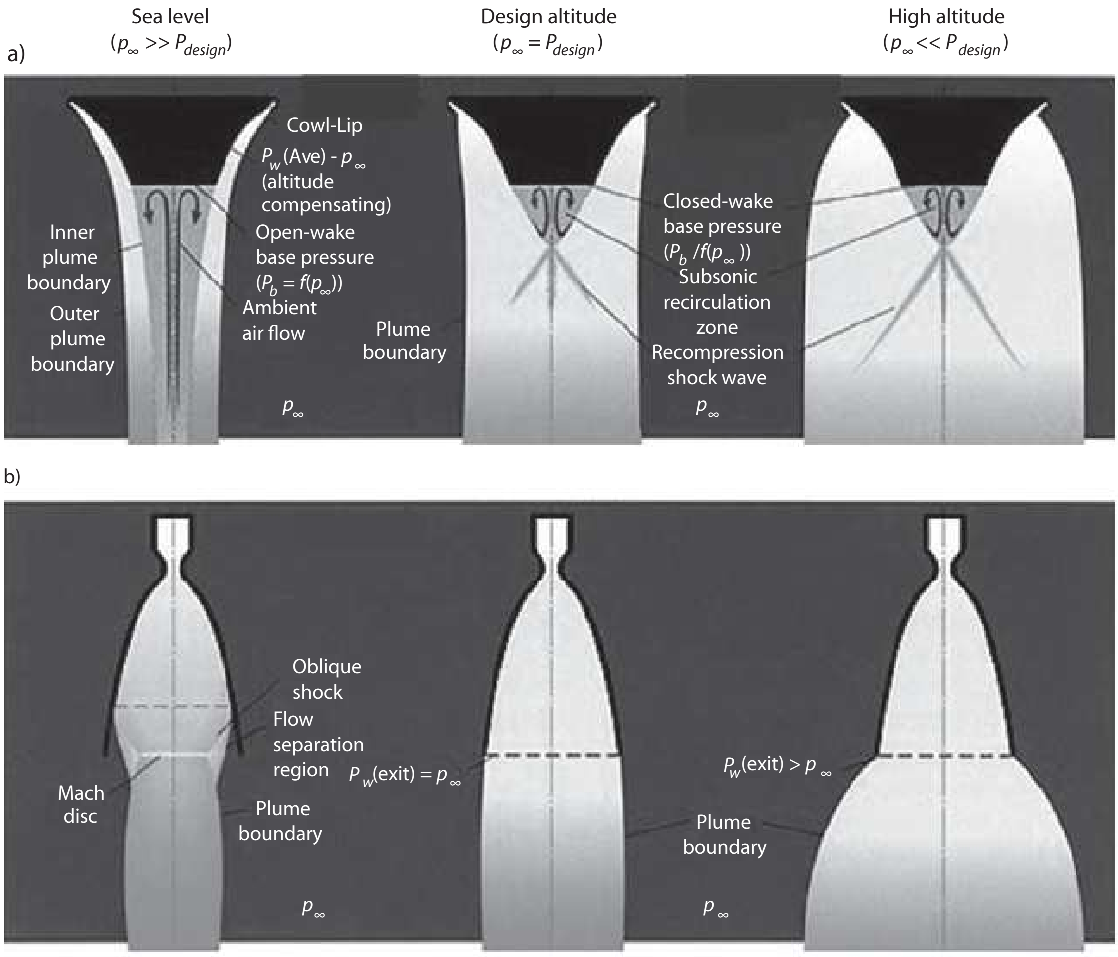

Fig. 4.31 Comparison of a) conventional and b) aerospike nozzle performance as a function of altitude. Source: AerospaceWeb.

forms one side of a "virtual nozzle," with the ambient pressure forming the second side (the "aero" portion of the aerospike name).

At low altitudes, the ambient pressure compresses the exhaust plume against the spike. As the vehicle ascends, the ambient pressure decreases, and the exhaust plume is free to expand; this means that the nozzle behaves as if it contained an "altitude compensator," in that the size of the virtual nozzle automatically changes as the ambient pressure changes. Note, however, that an aerospike nozzle is not a panacea: as seen in the middle figure of Fig. 4.31b, there will still exist only one altitude where an aerospike will operate at maximum efficiency.

Several versions of the aerospike exist, although the linear configuration of the X-33's XRS-2200 engine—in reality a collection of Rocketdyne J-2S hardware outfitted to a custom spike (see Fig. 4.32)—is arguably the most well-known. The linear aerospike has the primary advantage of allowing several smaller engines to be "stacked" along the spike to attain the desired thrust levels, while providing steering inputs by individually throttling the engines. Another type of aerospike nozzle is known as the *toroidal aerospike*, shown in Fig. 4.33. For this configuration, exhaust is blown from a ring

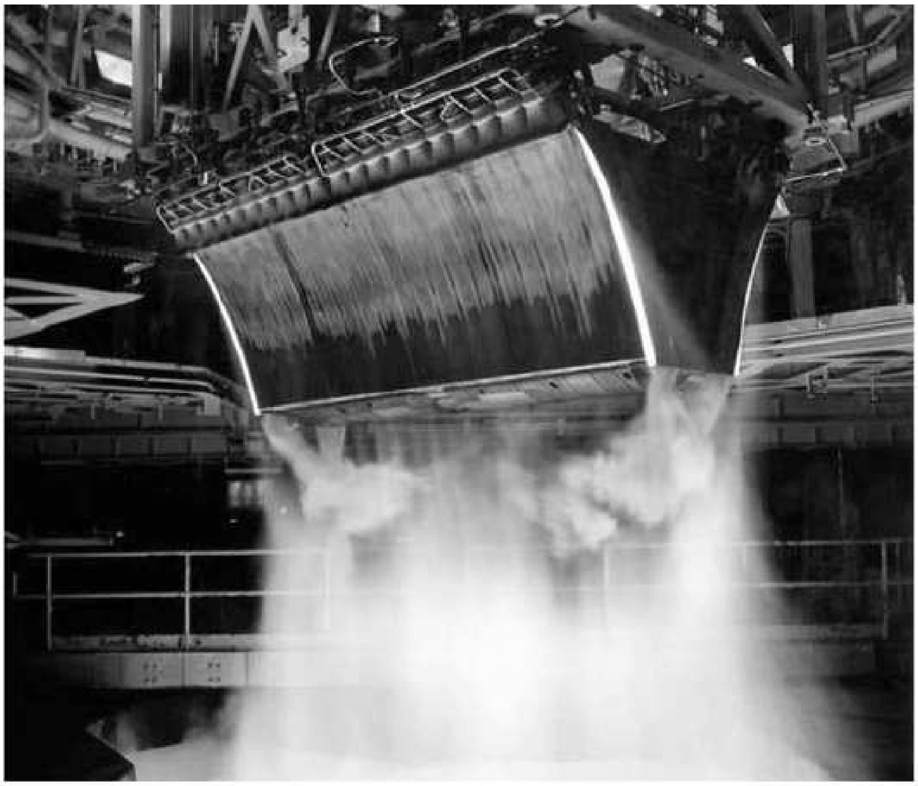

Fig. 4.32 Test-firing of XRS-2200 linear aerospike.

along the outer edge of the nozzle, and the central spike section operates in a fashion similar to a linear aerospike. This aerospike configuration was flight-tested by a joint industry/academic team (Garvey Spacecraft Corporation and California State University Long Beach) in Sept. 2003.

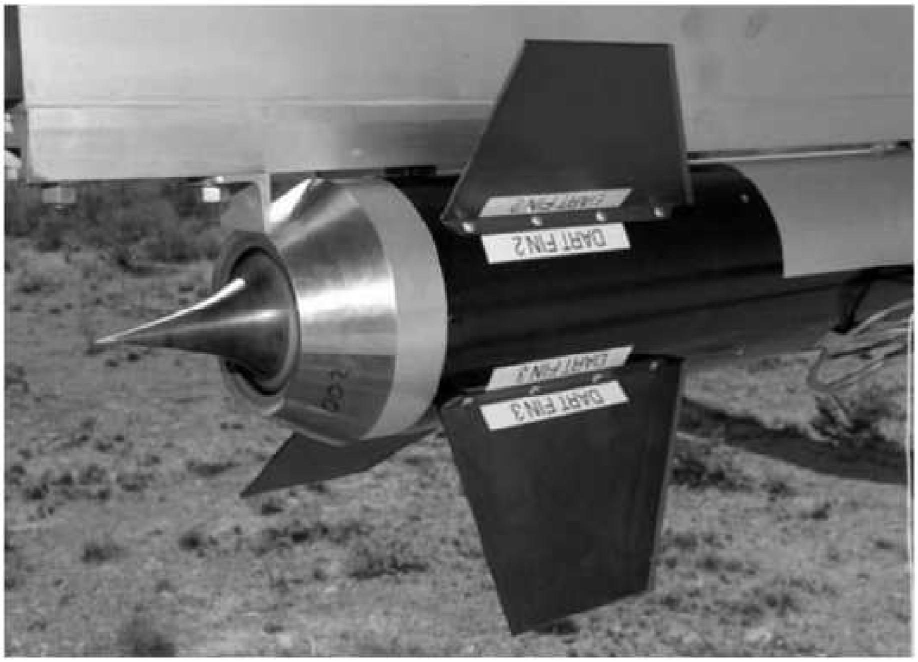

Fig. 4.33 Toroidal aerospike nozzle.

Despite the cancellation of the X-33 program, aerospikes remain an area of active research. Further successes came in 2004, with the successful tests of solid-propellant aerospikes conducted at NASA Dryden (now Armstrong) Flight Research Center. The rockets used in these flight tests reached altitudes of 26,000 ft and speeds of approximately Mach 1.5.

One of the most important recent milestones in the development of aerospike technology is the ARISE (Aerospike Rocket Integration and Suborbital Experiment) program from AFRL (Air Force Research Laboratory) program, focusing on the demonstration of a modular aerospike liquid engine with a truncated annular nozzle, which is then integrated into a prototype for suborbital flight. In many ways, the aerospike configuration lends itself well to modularity (i.e. repeated use of identical or similar parts, as opposed to conventional rocket engines which utilize a large number of individual and unique components), and ARISE focuses on low-cost engine solutions that leverage existing technologies. The highly-instrumented nozzle is designed to measure wake behavior, and the plume measurements will be used to validate CFD models and aerospike design tools.

Fig. 4.34 The ARISE aerospike engine on the ABL (left) and INVOCON (right) models. Left: Courtesy ABL; Right: Courtesy Guy Norris, Aviation Week & Space Technology.

It is hoped that ARISE achieves the first flight of a truly representative aerospike engine, the efforts of which will help mature the technologies necessary for the next generation of launch vehicles. Any new design paradigm creates uncertainties related to performance, reliability, cost, etc. that become barriers to general acceptance by an industry. Development efforts such as ARISE help mature technologies and reduce risk and costs, bridging the gap between the experimental and the tried-and-true. AFRL has awarded separate agreements to ABL Space Systems and Invocon, Inc. to develop flight demonstrators for ARISE; subscale models of these two flight test vehicles are shown in Fig. 4.34.

Further aerospike developments have been achieved by Pangea Aerospace in Spain. Their efforts have focused on the development of the DemoP1 engine, a pressure-fed metholox (liquid methane + liquid oxygen) engine that incorporates additively manufactured (3D printed) parts. The DemoP1 is intended to serve as the basis for the ARCOS engine – a booster-class, reusable aerospike engine that will power the MESO reusable launch vehicle. A solid model of the DemosP1 is shown in Fig. 4.35. To date, the igniter for the DemosP1 has been hot-fired, as shown in Fig. 4.36. While aerospikes might once have been a technological curiosity, it is clear that multiple efforts are well on their way to making this engine type a viable, sustainable option for designers.

Fig. 4.35 The DemosP1 aerospike engine. Courtesy: Pangea Aerospace.

4.9 Hybrid Rockets

A hybrid rocket engine is one that uses propellants in at least two different phases; typically, one propellant is solid and the other is either a liquid or a gas, but other combinations have been used. A hybrid rocket is shown schematically in Fig. 4.37.

The simplest form of a hybrid rocket is a pressure vessel containing the oxidizer, combustion channels along the fuel, and an ignition source. Combustion occurs almost entirely along a diffusion flame adjacent to the

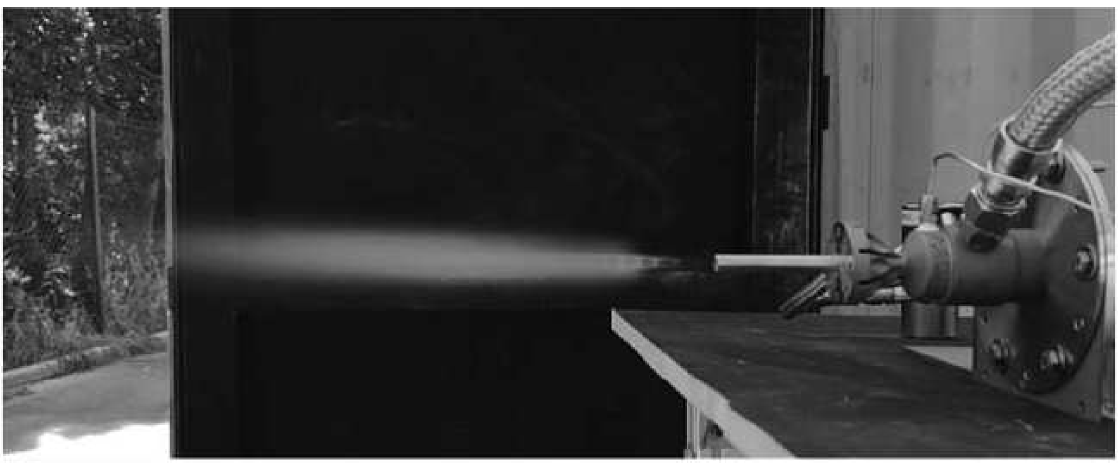

Fig. 4.36 Hot-fire testing of the DemosP1 igniter. Courtesy: Pangea Aerospace.

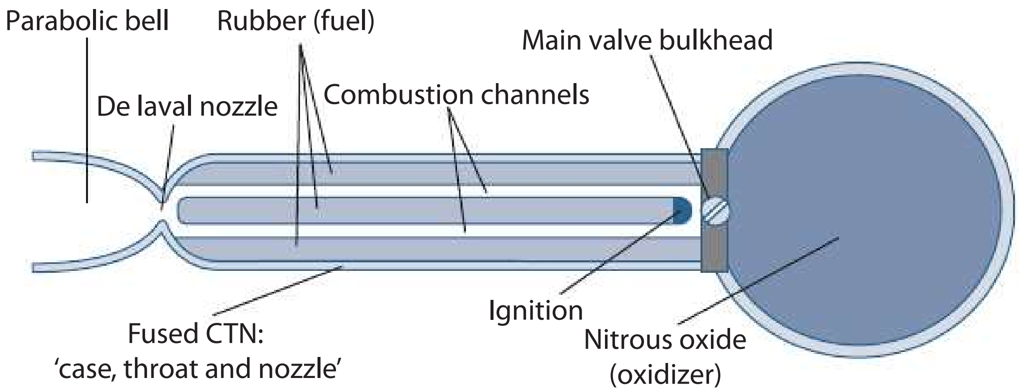

Fig. 4.37 A hybrid rocket engine. Source: Scaled Composites.

surface of the solid propellant. Commonly, the liquid propellant is the oxidizer and the solid propellant is the fuel. This permits the use of solid fuels such as hydroxyl-terminated polybutadiene (HTPB) and paraffin wax, into which fuel additives such as metal hydrides can be integrated. Other common fuels include polymers, cross-linked rubbers, or liquefying fuels. Depending on the propellants used, a hybrid rocket can avoid some of the disadvantages of solid-propellant motors (e.g., lack of means to control burn once initiated), while also avoiding some of the disadvantages (e.g., plumbing and mechanical complexity) of liquid-propellant engines. Hybrid rockets have one unique advantage over other configurations: because the propellants are two different states of matter, it is difficult for them to mix intimately, and thus the failure modes of a hybrid rocket tend to be more benign. Hybrids can also be throttled, although the specific impulse of hybrid rockets tends to be between 250 and 300 s; modern hybrids circumvent this issue through the use of metallized fuels and have demonstrated specific impulses on the order of 400 s.

Hybrids also exhibit some unique disadvantages, the most critical of which is known as an oxidizer–fuel shift (O–F shift), caused by the rate of fuel production to oxidizer flow changing as the solid grain regresses. Additionally, the use of fuels with a low regression rate (the speed at which the solid fuel recedes during combustion) will usually require a fuel grain with multiple combustion channels, which can contain structural deficiencies.

There are many possible ways to combine solid, liquid, and gaseous propellants defined as hybrid rockets. Several of these possibilities are shown in Fig. 4.38. Types a) and b) in the figure are the most common: liquid oxidizer/solid fuel and solid oxidizer, liquid fuel.

Designing a large (orbital booster–scale) hybrid rocket would also present the need to use turbomachinery to pressurize the oxidizer (or suffer increased vehicle weight from a thick-walled tank), which must obviously be powered in some fashion. In a liquid-propellant engine, this is done via one of the power cycle methods discussed previously. In a hybrid, such a pump would need an external power source or a monopropellant (such as hydrogen peroxide or nitromethane) that can be used to drive a power turbine; however, these oxidizers are less efficient than liquid oxygen, which cannot be used to power a turbopump. A secondary fuel would likely be needed to power the turbomachinery, which in turn would require its own tank and plumbing and decrease the vehicle's performance.

Successes have been had in the field of hybrid rocket research. For instance, the rocket that powered SpaceShipOne was a hybrid powered by nitrous oxide and HTPB. A breakaway view of this rocket is shown in Fig. 4.39. Hybrid rockets have even been considered for use as the strap-on boosters for the Space Shuttle, as shown in Fig. 4.40. For more information on the Space Shuttle SRB study and on different types of hybrid rockets, the reader is referred to Zurawski and Rapp [12].

Two additional types of hybrid rockets merit particular consideration: that of the gas generator hybrid and liquid-augmented solid rocket motor (LASR), both developed by Exquadrum and both of which have been demonstrated at scale. These two technologies address a combustion characteristic of classical hybrids wherein the flame front is similar to a candle: heat from the flame zone vaporizes fuel, which then contacts the oxidizer and combusts; and much like a candle's characteristic flicker, a classical hybrid motor suffers from an extreme amount of combustion instability. Specifically, nothing with a classical hybrid's design serves to anchor the flame, which is subsequently free to "wander" and exacerbate this combustion instability. Unstable combustion leads to fluctuating chamber pressure, which then manifests as a thrust oscillation, similar to the "pogo"

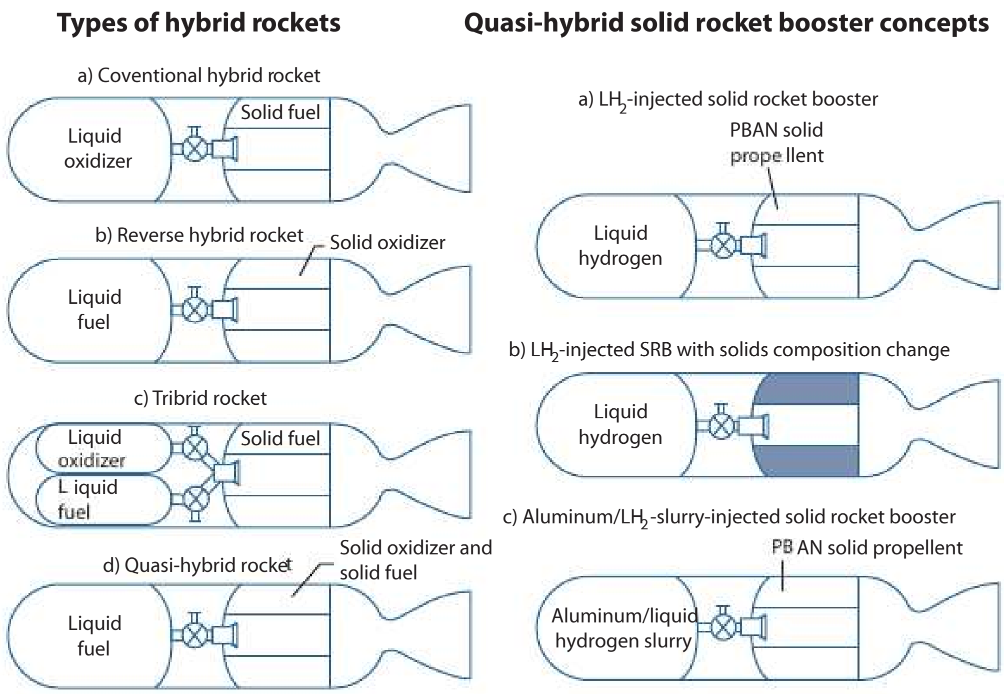

Fig. 4.38 Types of hybrid rockets. Courtesy NASA [12].

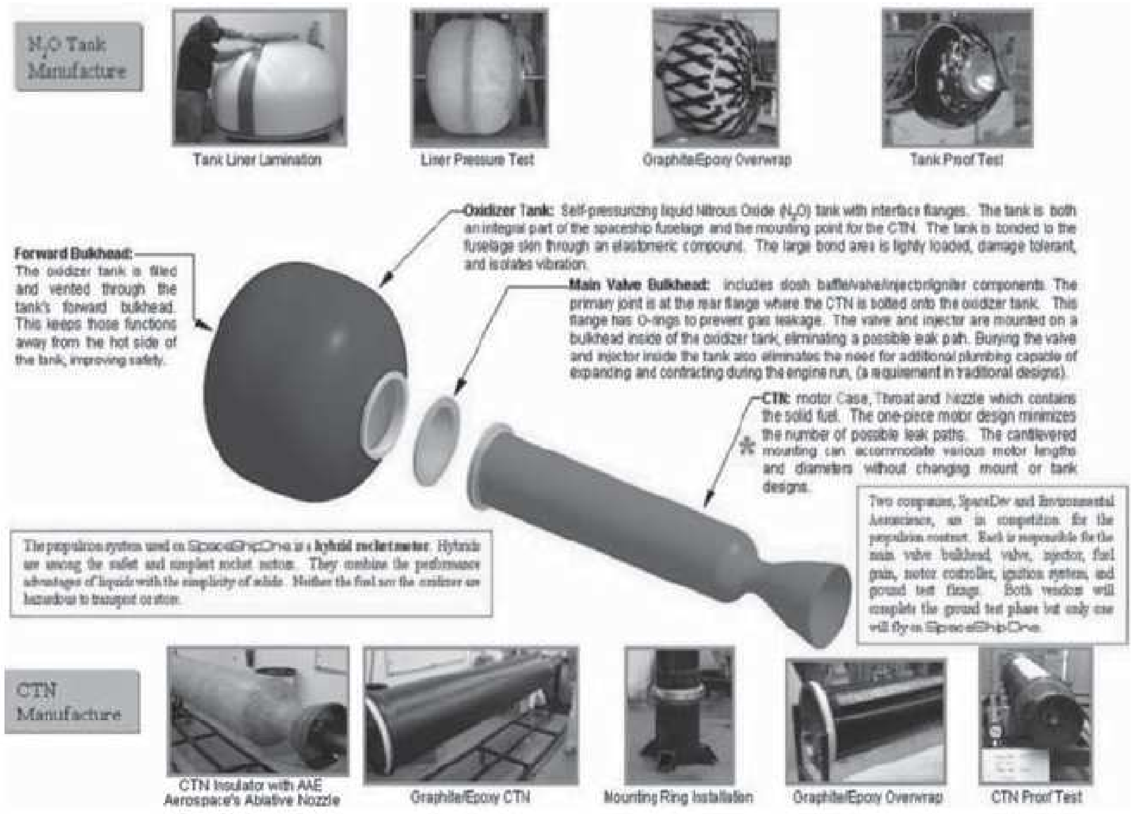

Fig. 4.39 Details of the SpaceShipOne hybrid rocket. Source: Scaled Composites.

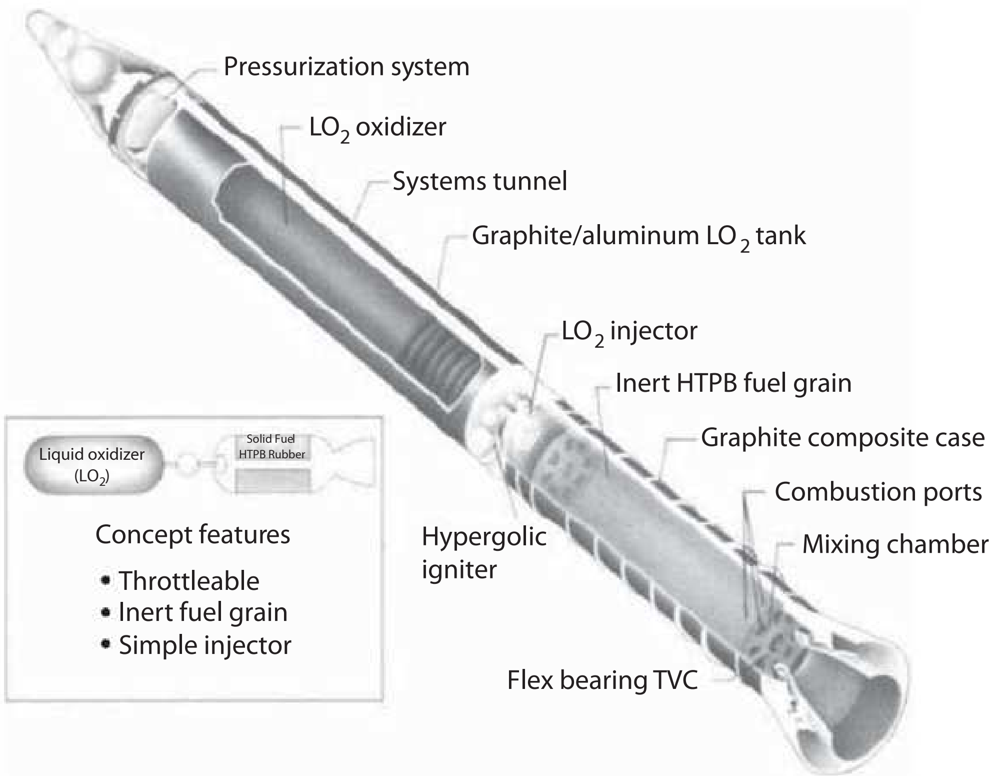

Fig. 4.40 Concept of a Space Shuttle hybrid rocket strap-on. Source: [7].

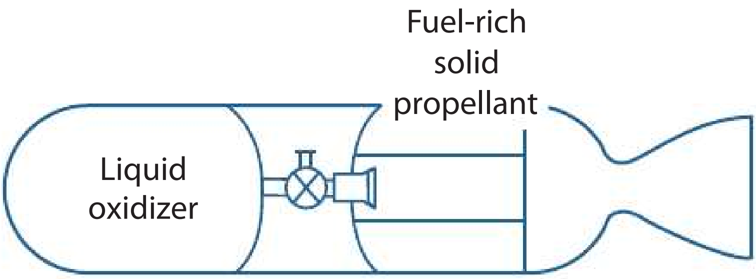

Fig. 4.41 The gas generator hybrid motor. Source: Exquadrum.

phenomenon that occasionally plagues liquid engines. There are several YouTube videos that go into detail regarding examples of combustion instability, including a PBS "Nova" special [13], archival NASA engine film footage from 1965 [14], and an example of a methalox engine exhibiting a low-frequency instability known as "chugging" [15].

The gas generator hybrid, shown in Fig. 4.41, shows some similarities to a classical hybrid, save that the fuel grain burns like a solid propellant; this provides excellent flame holding capability, and thus high combustion stability. For combustion and mass fraction efficiency, LOx is usually used for these types of engines, resulting in high energy density. A gas generator hybrid demonstrator, 36 inches in diameter and producing 60,000 lbf of thrust, was test-fired in January of 2013 (Fig. 4.42).

Fig. 4.42 Gas generator hybrid rocket motor test firing. Source: Exquadrum.

The LASR hybrid (Fig. 4.43) features a liquid monopropellant and a solid propellant grain structure, which serves as the catalyst bed for the monopropellant. The high temperature and combustion byproducts of the solid propellant drive the decomposition and combustion of the monopropellant. Traditionally, a catalyst bed for a monopropellant is inert and is accounted for as structural mass, adversely impacting the thrust-to-weight ratio of the engine and therefore the launch vehicle itself. With the LASR architecture, the catalyst bed is itself a propellant, and thus contributes to the output and efficiency of the engine, increasing the engine's specific impulse and the launch vehicle's overall performance. LASR hybrids also allow for very deep throttling. A LASR demonstrator test-firing is shown in Fig. 4.44; this demonstrator was 32 inches in diameter, although the thrust output for this test is classified.

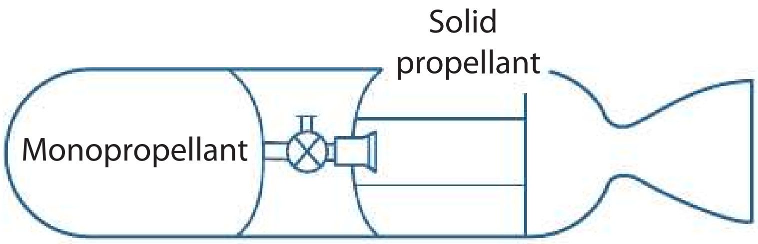

Fig. 4.43 Liquid-augmented solid rocket (LASR) hybrid. Source: Exquadrum.

Another advantage of hybrids is in the cost of propellant. Consider the costs shown in Table 4.15 reproduced with data from [16] and adjusted to 2020 constant dollars. It is immediately apparent that the propellants most likely to be used in a hybrid rocket are, far and away, also the least expensive. Although the performance of hybrids may not necessarily exceed that of other types of rockets, and as we show in Chapter 17 that the cost of propellants for a launch vehicle is almost negligible compared to other costs, the long-standing desire to drive down the launch cost per kilogram of payload may drive future launch vehicles increasingly toward hybrid rockets. This is especially likely in the commercial world, where "cash is king," and innovation is often required to directly influence the bottom line.

Fig. 4.44 LASR hybrid test firing. Source: Exquadrum.

Table 4.15 Propellant Costs, 2020 Constant Dollars.

Propellant Cost	US$/kg
Liquid hydrogen (LH_2)	10.65
Liquid oxygen (LOX, LO_2)	0.31
Kerosene (RP-1)	4.76
Dinitrogen tetroxide	130.87
Hydrazine (N_2H_4, UDMH, MMH, Aerozine 50)	505.64
Solid propellant (typical)	11.54

References

[1] Kuo, K. K., *Principles of Combustion,* Wiley-Interscience, New York, 2005.
[2] Kuo, K. K., and Acharya, R., *Fundamentals of Turbulent and Multi-Phase Combustion,* Wiley, New York, 2012.
[3] Turns, S. R., *An Introduction to Combustion: Concepts and Applications,* McGraw-Hill, New York, 2011.
[4] Sellers, J., Astore, W., Giffen, R., and Larson, W., *Understanding Space: An Introduction to Astronautics,* Pearson, Upper Saddle River, NJ, 2007.
[5] Ley, W., Wittman, K., and Hallmann, W., *Handbook of Space Technology*. AIAA/John Wiley & Sons, Reston, VA, 2009.
[6] Leondes, C. T., and Vance, R. W., *Lunar Missions and Explorations,* John Wiley & Sons, New York, 1964.
[7] Turner, M. J. L., *Rocket and Spacecraft Propulsion,* Praxis, Chichester, UK, 2009.
[8] Sutton, G. P., and Biblarz, O., *Rocket Propulsion Elements,* John Wiley & Sons, New York, 2001.
[9] Ordway, F., Gardner, J., and Sharpe, M., *Basic Aeronautics,* Prentice-Hall, Englewood Cliffs, NJ, 1962.
[10] Szatkowski, G., et al. "Centaur Extensibility for Long Duration," AIAA Space 2006, paper 60196.
[11] Riley, F., and Sailor, J., *Space Systems Engineering,* McGraw-Hill Inc., New York, 1962.
[12] Zurawski, R. L., and Rapp, D. C., "Analysis of Quasi-Hybrid Solid Rocket Booster Concepts for Advanced Earth-to-Orbit Vehicles." NASA Technical Paper TP-2751, August 1987.
[13] PBS, "Apollo's Daring Mission," *Nova,* https://www.youtube.com/watch?v=DjWiuMIGVEs [accessed 14 August 2022].
[14] NASA Marshall Space Flight Center, "NASA H-1 Engine Film Report 1965 (archival film)," https://www.youtube.com/watch?v=z4dOJGY5a7I [accessed 14 August 2022].
[15] Astromotive.Space, https://www.youtube.com/watch?v=9VKuhRFBnhU [accessed 14 August 2022].
[16] Koelle, D. E., "Economics of Fully Reusable Launch Systems (SSTO vs. TSTO Vehicles)," 47th IAF Congress, Beijing, 7–11 Oct. 1996.

4.10 Example Problems

1. A spacecraft has the properties listed in the table below. Calculate Δv, exhaust velocity, total impulse, and propellant mass flow rate.

Item	Value
M_0	3,200 kg
ζ	0.25
Burn time	3.35 s
Δp (change in momentum)	73,500 kg m/s
I_{sp}	275 s

2. A liquid oxygen–liquid hydrogen (hydrolox) motor produces 44.5 kN of thrust while operating at a chamber pressure of 6.895 MPa and a mixture ratio of 3.40. The exhaust products have a ratio of specific heats of 1.26 and a temperature of 2,689 K. Assume the motor operates at an altitude where the freestream pressure is a constant 9,500 Pa, and that the actual specific impulse is 96% of the theoretical value. Calculate:
   a) The speed of the exhaust stream
   b) Propellant mass and mass flow rate
   c) Nozzle exit area for optimal expansion
   d) Total propellant mass for 3 min. of burn time
3. A rocket engine uses RP-1 propellant to produce 9,000 N of thrust with an exit velocity of 1,250 m/s and will have a burn time of 67 s. Helium gas ($R = 2{,}077$ J/kg-K; $\gamma = 1.66$) is used as a pressurant and is pressurized to 14 MPa. The ambient temperature is 297 K. Calculate the mass of pressurant gas needed to pressurize the RP-1 tank to 3 MPa. Assume 1.2% residual propellant and 3% residual pressurant.
4. A propellant combination has a molecular mass of 23 kg/kmol and a specific heats ratio $\gamma = 1.24$. The combustion chamber temperature and pressure are 3,400 K and 6,900 kPa with $P_e = 101.3$ kPa (1 atm). The mass flow = 100 kg/s and the engine's exit diameter D_{Exit} is 0.62 m.
   a) Find the exhaust velocity v_e (m/s) at sea level.
   b) Find the *effective* exhaust velocity c (including pressure effects), the I_{sp}, and the thrust T at sea level.
   c) Find the exhaust velocity v_e (m/s) at altitude 9,150 m, where $P_{\text{atm}} = 37.88$ kPa.
   d) Find the *effective* exhaust velocity c, the I_{sp}, and the thrust T at 9,150 m altitude.
   e) Find the *effective* exhaust velocity c, the I_{sp}, and the thrust T in space.
   f) What is the theoretical maximum value of v_e and I_{sp}?
   g) Does thrust typically *increase* or *decrease* as altitude in an atmosphere increases? Explain.
5. A launch vehicle has a liftoff T/W of 1.5, a propellant mass fraction $\zeta_p = 0.9$, and $I_{sp} = 260$ s.
   a) Find the time to burnout t_b in seconds.
   b) Find the T/W at burnout, assuming constant thrust.
6. The S-II (second) step of the *Saturn V* had a very small structural mass fraction, because it was the last step designed of the three, and had to meet

very stringent mass requirements. Since it had such an efficient structure, it is attractive to consider it alone as a high-performance vehicle when Δv performance is calculated with the rocket equation. In actual operation, the S-II's five J-2 engines burned together until such time when the center engine was shut down to limit peak acceleration.

Assume that the S-II had the following characteristics:

Initial mass $m_0 = 480$ T (T = tonne = 1,000 kg), inert mass $m_s = 36$ T, $T = 5{,}100$ kN total, J-2 engine vacuum $I_{sp-vac} = 425$ s. Use $g_0 = 9.80665\ \mathrm{m/s^2}$.

a) Calculate the S-II's burn time t_b in seconds, assuming all five engines burned all the way to burnout and ignoring the effect of exhaust pressure.

b) Determine the maximum payload (kg) that could be delivered to a velocity of 9,150 m/s using this step as a single-stage launch vehicle.

c) Comment on your results for the amount of thrust available at sea level. Extra Credit: determine $I_{sp-\mathrm{sea-level}}$ (s), and calculate the sea level thrust value.

d) Determine liftoff T/W ratio. Ignoring the fact that the J-2 engines were optimized for high-altitude operation, could the S-II work as a launch vehicle? Comment on the situation, and explain why or why not.